IEEE Access
Multidisciplinary ⋮ Rapid Review ⋮ Open Access Journal

Received April 22, 2021, accepted May 16, 2021, date of publication May 21, 2021, date of current version June 2, 2021.

Digital Object Identifier 10.1109/ACCESS.2021.3082858

A Review of Knowledge-Based Defect Identification via PRPD Patterns in High Voltage Apparatus

TOHID SHAHSAVARIAN[1,2], YUE PAN[3], ZHOUSHENG ZHANG[3], CHENG PAN[4], (Member, IEEE), HADI NADERIALLAF[5], (Member, IEEE), JIM GUO[6], (Senior Member, IEEE), CHUANYANG LI[1,2], AND YANG CAO[1,2], (Senior Member, IEEE)

[1]Department of Electrical and Computer Engineering, University of Connecticut, Storrs, CT 06269, USA
[2]Electrical Insulation Research Center, Institute of Materials Science, University of Connecticut, Storrs, CT 06269, USA
[3]School of Electrical Engineering, Shanghai University of Electric Power, Shanghai 200090, China
[4]School of Electrical Engineering, Wuhan University, Wuhan 430072, China
[5]Department of Electrical, Electronic, and Information Engineering "Guglielmo Marconi", University of Bologna, 40136 Bologna, Italy
[6]Altanova, TECHIMP U.S. Corporation, Alpharetta, GA 30022, USA

Corresponding authors: Yang Cao (yang.cao@uconn.edu) and Chuanyang Li (lichuanyangsuper@163.com)

ABSTRACT Partial discharge (PD) as one of well-known signatures of defects in the insulation system of high voltage equipment has been studied over eight decades. It is of a great interest to power grid operators and owners to identify and distinguish local weak spots in insulation system of the key components of power system by using the obtained PD information to make timely decision thus to avoid any unexpected failures in the system. This article reviews the research progress of PD in high voltage apparatus, including motors and generators, cables, transformers and gas insulated equipment, with attempts to assess the severity of different types of PD initiating defects as well as key PD features that can be selected for classifying defects. Experimental and on-site test results for each type of discharge and defect associated are summarized and discussed. Also, development of these defects during operation of equipment caused by changes in physical and chemical parameters of defect and/or insulation, and its impact on phase-resolved PD pattern variation are thoroughly explained. It is expected that this paper can provide a comprehensive guideline for PD data analysis of available PD information extracted by conventional PD acquisition instruments for both engineers and asset managers of high voltage apparatus.

INDEX TERMS Partial discharge (PD), high voltage motor, power cable, power transformer, GIS, GIL.

I. INTRODUCTION

Decision making on the needs of maintenance, replacement or repairing of a high voltage apparatus so as to avoid costly unplanned loss of operation due to premature failure of insulation remains a challenging issue that demands proper condition assessment of the electrical insulation of various components in service. Depending on the equipment and type of insulation system used in its design configuration, cost of the in-service actions could be significantly higher for utilities. Therefore, there is a dire need of timely identification of defect and life-time estimation based on the severity of defect.

The associate editor coordinating the review of this manuscript and approving it for publication was Zhouyang Ren.

Partial discharge (PD) as one of the well-known signatures of the presence of defects in insulation system has been extensively investigated over eight decades. Researchers have been focusing on the correlations between the detected PD signatures and type of defect, intensity of electrical stress, location of defect and insulation remaining life-time estimation. Nonetheless, available expert knowledge and techniques are not accurate and sufficient for reliable assessing of insulation condition and, upon which, the corresponding decisions making.

However, extensive investigations on PD patterns for different types of defects by researchers over generations provide well-defined features of patterns which can be summarized and utilized to distinguish the defects

without requiring complicated feature extraction and data processing techniques. Aim of this paper is to present a sufficient summary of major findings in existing types of defects in high voltage equipment and their corresponding phase-resolved PD (PRPD) patterns, and illustrate the impact of other parameters on changes in patterns. Section 2 presents different types of defects introduced for this equipment as well as the impact of PD activities initiated by these defects on insulation system performance and lifetime of equipment in service. Section 3 delineates categorized PD patterns corresponding to the introduced defects. Experimental and on-site test results obtained by the different research groups for the defects are shown and discussed; and key recognized PD patterns for each case are introduced. This work can be as a useful reference and guideline for insulation system diagnosis for PD pattern data analysis recorded by available PD acquisition and measuring instruments.

II. INFLUENCE OF PDs ON HV APPARATUS

A. HV MOTORS AND GENERATORS

HV motors and generators generally refer to rotating machine with a rated voltage higher than or equal to 1000 V. During the operation, the insulation suffers from electrical and mechanical stresses which could damage the machine and cause in some cases an inestimable economic loss to the electricity production and power systems. In most cases, the insulation failures are caused by aging of stator windings. The stator winding insulation is affected by heat, electrical, mechanical and environmental aging during the operation, which generate defects that support the PDs and in turn accelerate the aging rate. The most common type of PDs that occur in stator windings are internal discharge, slot discharge, corona discharge, phase-to-phase discharge, and spark discharge [1], [2].

1) INTERNAL DEFECTS

Internal defects are generated by air gaps in the main wall insulation of the stator windings during the manufacturing process to initiate the internal discharges which cause further damage to the insulation. Most of the generators and motors experience internal discharge inside the main wall insulation of stator windings at their rated voltage. The epoxy mica insulation has been manufactured as the main wall insulation, which can withstand the normal internal discharge activity for more than 40 years while maintaining excellent electrical properties [3]. Therefore, the internal PD does not attract much of the attention due to the less damage compared with other types of PDs. However, in case of large internal voids, the amplitude of internal PDs sometimes could reach a level which may overcome the PDs caused by other harmful PD sources. Also, due to an uneven size distribution of the internal air gaps, the related internal PD frequency can reach a wide band range which may cause troubles in the identification of PD types during online monitoring process. Meanwhile, it has been reported that in some cases, the internal

FIGURE 1. Stator windings aged for a long time due to internal discharge [5].

PD causes abnormal destructive forces, sometimes resulting in delamination of the inter-turn insulation and the main insulation [4]. Figure 1 shows the stator bars from a 6kV motor after 20 years of service with serious damage observable in the main wall insulation, which is due to internal PDs [5].

2) SLOT DEFECTS

The slot defect occurs due to the discharges in the air gap between the stator core slot and the main wall insulation of the stator coils and/or bars [6]. The aging of the insulation layer prevents normal heat conduction, which increases the local temperature of winding, intensifies slot discharge activity, and ultimately shortens the operation lifetime of the machine. Figure 2 shows the damage of the stator winding surface due to the slot discharges [7], [10], [13], [14]. The consequences of the slot discharges in the defect location are summarized as follows:

FIGURE 2. (a) Deposition of oxidized powder caused by slot discharge [10]. (b) A slot coil damaged to vibration abrasion [13].

- The loose stator bars in the core slots could take place due to the vibration during operation. This case is usually caused by an improper installation but may also be due to years of insulation shrinkage during material and thermal aging. If a bar begins to vibrate, the movement of the bar wears the slot conductive coating and the main wall insulation and initiates the PD inside the air gap, which results in depositing iron oxide powder in the depression of the insulating surface [7]. Figure 2(a) shows the deposition of the oxidized powder after a stator winding of an 8 kV air-cooled generator was aged for 1200h due to the slot discharge at 16 kV AC voltage. Figure 2(b) shows that the semi-conductive layer in

the straight portion has been severely worn, and the surface has visible signs of aging due to vibration and wear.

• In the case that the conductive coating is isolated from the grounded core by the air gaps due to vibration or unsuitable installation, the conductive coating cannot be effectively grounded and thereby discharges would occur inside these air gaps. Insulation aging caused by slot discharge oxidizes dielectric surface, which in turn affects the process of the slot discharge [8]. Another case is the poor contacting of the gap conductive coating, forming a non-conductive local area. Under high pressure operation, a discharge occurs between the bar and the core. The damaged area of the coating becomes larger over time, and the intensity of PD increases. In addition, slot discharge produces ozone, which in turn causes nitric acid to damage the motor [9].

Studies regarding influencing factors on slot discharges, including temperature, humidity, gap distance and abrasion have been conducted worldwide, which can be reviewed in Figure 3.

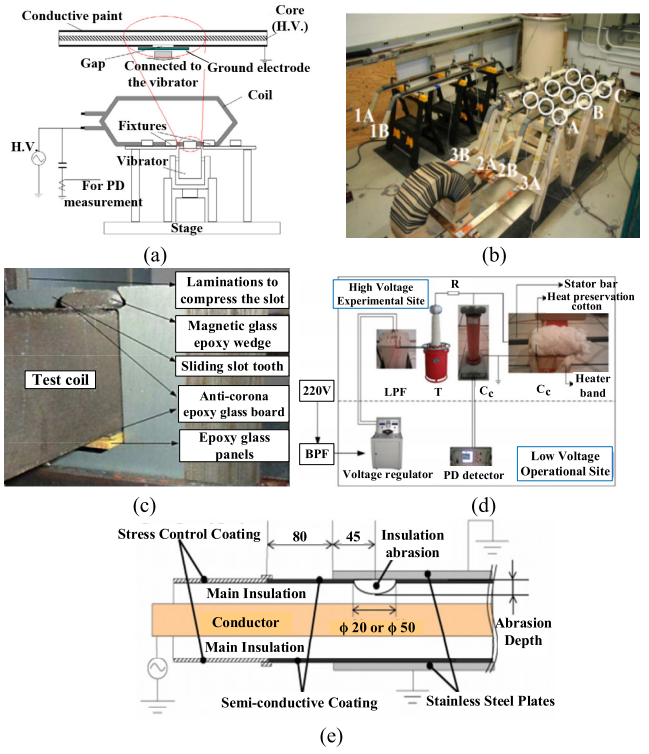

FIGURE 3. (a) K. Wu designed slot discharge experimental platform [15]. (b) Discharge model designed by Léveaque [9]–[11] and Hudon *et al.* [12]. (c) C. Li designed slot discharge experimental platform [13]. (d) A. Kang designed slot discharge experimental platform [16]. (e)Tank discharge experimental platform designed by Joyo *et al.* [17].

3) DEFECT IN SLOT EXIT

This type of defect at the junction of the semiconductor coating and the stress grading paints at the end of stator windings initiates corona discharge [14]. At the exit end of the stator winding, the electric field distribution is extremely uneven. Under the action of the volumetric capacitance, the current distribution per volume unit is uneven, and the air gap

FIGURE 4. (a) Corona discharge at the slot outlet causes single phase ground fault on a 10kV three-phase asynchronous motor [18]; (b) Marks of corona discharge at the slot exit of a 2000kW/6kV high voltage motor [5].

is more prone to corona discharge where the electric field is higher. The deposition of iron oxide white powder in the gap at the joint have been determined as the source of such PD, which can be visually inspected (Figure 4). Such PD does not develop into a more severe spark discharge because of the blocking of the insulating medium. However, it is more likely to occur at the air gap at the exit end of the stator winding which is stronger than the corona discharge between the stator winding and core because of extremely uneven electric field distribution at the exit end of the stator winding.

4) INTER-PHASE DEFECTS

This type of defect occurs between two stator bars and/or coils or neighboring winding surfaces in high-voltage motors [9]. The copper core inside the stator winding has an induced potential to ground, which is transferred to the insulating surface by a capacitive effect. When the potential difference of the adjacent winding insulation surface is sufficiently large and the field strength generated by the electric potential exceeds the breakdown field strength of the air gap, the gas molecules are ionized to generate an electron avalanche, which finally leads to PD between phases. Such discharge decreases the insulation properties and also produces a white powder on the insulation surface. To avoid such PD, sufficient air gap must be left between the stator and the windings during installing the windings. Figure 5 shows photographs of the fault after bar-to-bar discharge. Experimental model of bar-to-bar discharge can be found in [3], [16] [17].

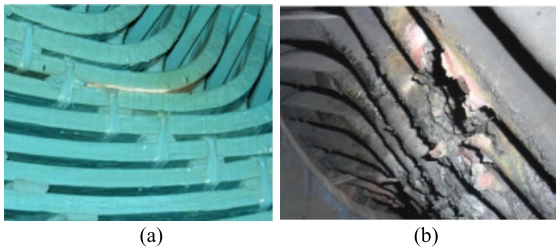

FIGURE 5. (a) Bar-to-bar discharge between stator coils of different phases of the motor(≥6kv) [19]; (b)bar-to-bar discharge between stator bars of 10kV motors [18].

5) SPARK EROSION

The vibration of the stator bars is the key initiation of spark discharge [21]. During normal operation, a loop current

passes radially through the core lamination and moves axially along the back of the stator core to the bar [22]. As the bar vibrates, the conductive coating on the surface of the bar will be separated from the core. The induction current loop in the semi-conducting layer on the surface of the bar is cut off and an arc is generated at the same time, eventually forming a spark discharge which destroys the main insulation very effectively. Compared to other types of discharge, spark discharges have more released energy and are more destructive to insulation. It is reported that it takes about 5 years from the occurrence of spark discharge to insulation failure [14]. A typical feature of spark discharge is the presence of dust and significant pitting after insulation layer degradation. Figure 6 shows a typical generator stator bar, having been in operation for ten years and suffering from the spark discharge and a stator bar surface damaged by vibration sparking [23]. Simulated vibration spark discharge needs to meet two conditions: the presence of current in the semi-conductive layer on the surface of the bar, and vibration [24].

FIGURE 6. (a) The fault scene of the spark discharge after the stator bar near the neutral point of the winding is removed, (b) Borescope images of the side of a stator bar surface damaged by vibration sparking [23].

B. HV CABLES AND ACCESSORIES

The main cable insulation, terminals, and joints are vulnerable segments of a high voltage cable to different types of PDs which have been studied widely over the past half-century. Depending on the discharge location, they can be categorized as corona, surface or internal discharges. Defects can be introduced during the process of manufacturing, transporting or assembling the power cables to induce electrical stress and PD. Also mechanical stresses (such as bending, tension, compression, vibration), thermal stresses (such as high current carrying condition and joule heating), and environmental stresses (such as moisture, chemicals, radiation) can result in oxidation, chemical decomposition, water and electrical trees, and space charge in the insulation [25], [26]. Moreover, different types of defects have different aging stages as well as propagation speed along the insulation which should be distinguished based on the obtained PD patterns. Different kinds of discharges in cable system have been illustrated in this section and corresponding PRPD pattern features have been discussed in section 3.2.

1) METALLIC PROTRUSION IN AIR

Protrusion defects in high voltage conductors adjacent to the air occur in transmission lines, switchboards, switchgears, and cable terminations where gas ionization due to the high electric field gradient initiates corona discharge. Generally, this type of discharge occurring in cable terminations are less harmful since discharge ionizes the air without interacting with cable insulation. Also, other reasons for the initiation of corona discharge are improper corona rings and connectors with protruding bolts [27]. However, this kind of discharge can be easily initiated and detected pattern be mixed with the patterns corresponding to the other type of severe defects.

2) SURFACE DEGRADATION

Dielectric surface damages are one of the major causes of insulation failure which are initiated by localized surface discharges and extends to the creepage discharges, flashovers and final breakdown of insulators and gas/solid interfaces in power system apparatus. It specially happens where outer insulation layer of the cable is damaged and/or where the screen is removed from insulation at cable joints and terminations. Ionized conductive path of discharge on the surface degrades the insulation which can be observed as carbonized track. Figure 7 shows an example of surface discharge initiated carbonized paths on the cable surface due to two main possible reasons: void between the joint insulation and the central conductor due to inadequate heat shrink, or excessive carving [28].

FIGURE 7. Carbonization inside the cable termination (left) [28], penetration track on the cable joint (right) [29].

In [27], different reasons for surface discharge in a hollow core cable termination have been described. Contaminants on the inner surface of the termination especially around the stress cone with higher electric field, and the moisture on the inner surface at temperatures lower than dew point can facilitate initiation of surface discharge. Long air gaps between insulation parts especially in cable splices and plug-in terminations, poor polishing of the outer semiconductor required for concave transition to the insulation and air gaps in this area can lead to the surface discharge.

3) INTERNAL DEFECTS

Internal discharge happens inside the insulation and is non-observable and more difficult to be detected and localized than other type of discharges. Different types of defects inside the insulation can initiate internal discharge as shown in Figure 8. Since each of these defects has its own specific

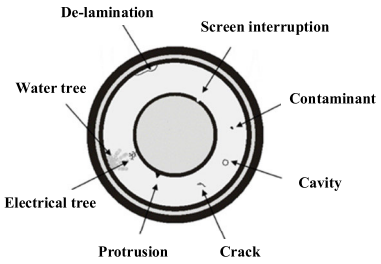

FIGURE 8. Different types of possible defect inside the insulation [30].

PD patterns, the cause and consequence of the major defect types are separately explained.

a: CAVITIES

Cavities are well-known type of internal defects which are created between the conductor and insulation (electrode bounded) or inside the insulation (insulation bounded). Intensified electric field inside these gas-filled voids due to difference in permittivity of gas and insulation material initiates internal discharges in these localized spots. Intensity of discharge and degree of risk depend on the size, shape, location of void, chemical compounds inside of gas and void wall, and voltage across the insulation (Figure 9). We have already studied impacts of these parameters on intensity of internal discharges using the proposed model for different aging stages and experimental results [31]–[33].

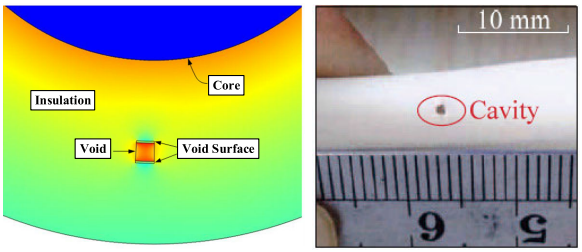

FIGURE 9. Schematic illustration of void inside the insulation (left) [31], experimental void model between EPR layers using steel ball (right) [33].

b: ELECTRICAL AND WATER TREES

One of main routes to cause failure of cable insulation is conductive electrical trees (ETs) initiated from where electric field intensifies around void wall, protrusions and cracks. Occurrence of PD within the developing tree branches lead to progression of tracks along the insulation. Shape of the formed trees hinges on the electric field intensity and permittivity of insulation material which is categorized into three groups as shown in Figure 10.

Stagnated tree is a dense branch tree restrained by insulation. ET can be initiated by an electrical stress such as over-voltage transients in the form of branch or bush like trees; however, bush-like tree can be converted into branch-like tree and lead to the ground electrode before final breakdown. In [35], it is shown that temperature and voltage level have significant impact on the progression of ETs in XLPE. Both branch-like and bush-like trees have been observed at lower voltages, while branch like trees were dominant type of tree forms at higher voltages. These trees are initiated earlier at higher temperatures but slower tree development at lower voltage at higher temperatures within the range of reported temperatures (50-90°C). Rationale behind this observation has not been thoroughly understood and delineated.

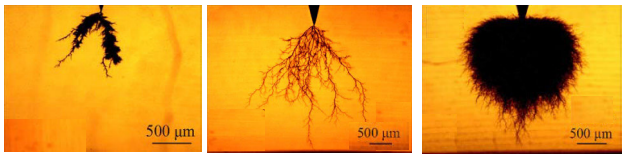

FIGURE 10. Possible ET shapes: (a) stagnated tree, (b) branch-like tree, (c) bush-like tree [34].

Presence of moisture inside the insulation around intensified electric field areas results in water trees (WTs) which have relatively slower propagation rate. Transient over-voltages can transform the WTs into ETs (Figure 11(a)), or ETs to WTs in the rare cases for service-aged cables (Figure 11(b, c)).

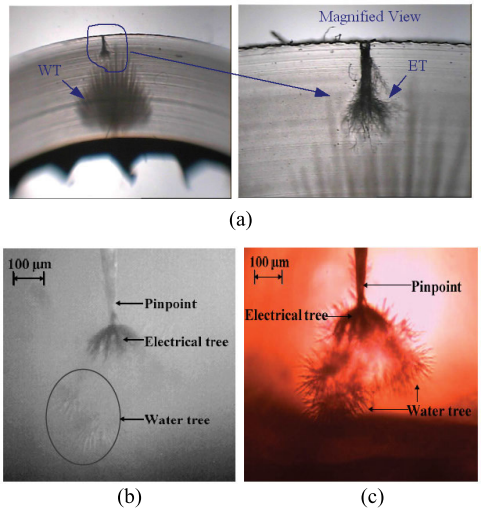

FIGURE 11. (a) Initiation of ET due to enhanced field around WT in XLPE [37], development of WT from ETs in XLPE observed by: (b) CCD camera, (c) low-powered optical microscope [38].

c: PROTRUSION, DELAMINATION AND CONTAMINANTS

Protrusions are one type of imperfection in cable system in the form of sharp points on high voltage conductor or ground sheath which can disrupt locally uniform electric field distribution and generate PD in intensified electric field regions. Those defects produced in joints or terminations and surrounded by air are less destructive, and generate corona discharges [39] in the air, while protrusions located on the conductor shield or insulator shield can degrade the insulation strength and generate electrical trees.

Delamination in cable splices and plug-ins can be a reason of surface discharge as explained before. Also, delamination of semiconducting screens caused by rough handling while installation can be a source of internal discharge and further treeing inside the insulation [37], [40], [41]. Contaminants and cracks as impurities inside the insulation can intensify the electric field locally and initiate treeing process and cause further degradation of insulation.

C. HV TRANSFORMERS

Power transformers are known as one of the most important equipment in power system with high maintenance cost [42]. Prior experience indicates that PD will not lead to severe insulation damage temporarily, but in a long time, it can gradually develop, and result in more serious insulation failures [43]. It has been known that the aging of insulating materials caused by consistent PDs often would be the result of long-term discharge process with lower intensity rather than intense discharges and short-term aging [44], [45]. It is observed that discharge frequency and the total discharge volume are at a very low level in the initial period, both of them grow slowly with the development of PD, afterwards, PD enters a rapid and irreversible development stage, with the further development of discharge, which finally results in breakdown [46].

In the paper insulated HV transformers, PDs begin at small pinholes penetrating the paper windings that are adjacent to the electrical conductor or outer sheath. As PD activity progresses, the repetitive discharges eventually lead to permanent chemical changes within the paper layers and impregnating dielectric fluid. Over time, partially conducting carbonized trees are formed. Sustained PD can lead to erosion of solid insulation and final breakdown [47].

In practice, it is usually preferred to allow a HV transformer to run under a PD level below 100 pC. However, it is suggested that its operation should be stopped when the PD level is over 100 pC to prevent further failure [44].

1) METALLIC PROTRUSION

Existing metallic parts on high voltage parts inside the oil of transformer or protrusions can generate corona-like discharges inside the oil similar to the discharge type discussed in other high voltage equipment for air [50]. Consequently, the dielectric strength of the oil gradually reduces, leading to plausible failure of the transformer [42]. Not only the shape and length of protrusion can affect the intensity of the discharge, but also the temperature, water content and other parameters of insulating oil can have significant impact on insulation strength and lifetime [51]–[53]. This kind of discharge is implemented in experimental platform using the needle-electrode configuration embedded in the oil (e.g. in [52]).

2) CAVITIES

Gas-filled cavities in solid electric insulation of transformers especially imperfectly impregnated paper caused by bad manufacturing process or ageing, besides air bubbles in oil resulted from nonlaminar oil flow or turbulent flow. Regarding the solid insulation, Kraft paper is extensively used in the insulation system of oil-filled power transformers. The dielectric properties of Kraft paper can be degraded if there is a void within the paper resulting from discharges inside the void through changing the dielectric strength of paper [54]–[56]. In addition, oil impregnated pressboard (OIP) is used widely as an insulation barrier in transformers. However, it has hygroscopic property and can absorb the moisture and deteriorate insulation property of OIP resulting from reduction of PD inception voltage (PDIV) for air-filled cavities. The reason of PDIV reduction is due to the increase in relative permittivity of OIP, ratio of permittivity of OIP to gas, and the electric field inside the cavity [57]–[59]. Therefore, the effect of moisture on PD characteristics of OIP is an important factor in insulation diagnosis and reliability analysis of a transformer [59]. Shiota *et al.* have investigated the behavior of bubbles in the oil and the effect of bubble size [60]. Also, Niasar *et al.* have shown bubble elongation and separation processes as given in Figure 12.

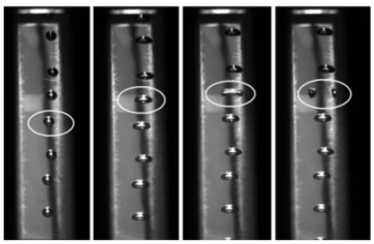

FIGURE 12. Elongation and separation of introduced bubbles inside the Nytro 10XN transformer-oil [61].

3) SURFACE DIGRADATION

The interface between solid and liquid insulation such as pressboard (or paper) and oil is often considered as a relatively vulnerable part of transformer insulation since lower electrical stress along the surface would be more harmful than the electrical stress across the insulation bulk [62].

For oil-paper insulation, although oil strength is relatively lower than the paper, the interface of oil-solid is more susceptible to degradation than oil [64], [65]. Failure due to surface discharge in power transformers in service has been reported in [44], [66]. There are many kinds of interfaces in HV transformers including the spacer between the winding layers, winding screen, insulating cylinder, and pressboard barriers between phases. The characteristics of surface PD mostly depend on the shape of the electrodes [67]. When the local electric field is increased by degradations like moisture, dielectric degradation, or winding deformation, discharge may occur along the paper interface. Initially, the discharge along the oil-paper interface would be in the form of PD. Sustained PD causes unrecoverable tracks and carbonized areas on the pressboard surface [68], [69]. This

FIGURE 13. (a) Tree-shaped discharge tracks on the: the pressboard barrier in a scrapped transformer [70], (b) two pressboards impregnated in MIDEL 7131 [69].

kind of dielectric degradation can lead to flashover along the surfaces, winding short-circuit, and even bushing explosion [44]. Figure 13 shows a surface tracking form on the pressboard surface inside the oil. There are substantial differences between different insulating fluids being used to fill HV transformers regarding the average PD levels. Mineral oil is accounted for the lowest PD levels compared to ester fluids. The highest PD values have been reported for the pressboard impregnated by synthetic ester surrounded by natural ester [71].

D. GAS INSULATED EQUIPMENT

Sulfur hexafluoride gas (SF_6) was introduced as the most promising insulating media in high voltage apparatus about half a century ago [73]. Although SF_6 insulated equipment is compact and well insulated, the high field strength inside enclosure makes it more sensitive to perturbations in presence of defects and contaminants which can be either insulating or metallic particles. These defects - especially the metallic particles - can intensify local electric field and result in PDs and lead to failure of the equipment. The installation cost and required maintenance time for this type pf equipment are higher than conventional high voltage components. Therefore, PD detection and defect identification with reliable methods and high fidelity sensors during the service are essential.

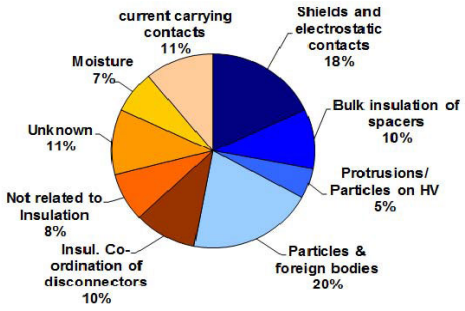

FIGURE 14. Statistics of occurring different type of defects in GIS equipment [75].

As can be seen in Figure 14 in a CIGRE report (WG 33/23.12 [74]), possibility of poor contact including flowed load current through contacts and failures due to shields and bad electrostatic contacts is 29%. Protrusions and particles over HV conductor, and particles and foreign objects cover 25% of dielectric failures in service.

1) FREE-MOVING METALLIC PARTICLES

This type of defect can be created through rubbing of different metallic parts during assembling, operation or installation and observed in different forms such as metal powders, flakes or large size solid particles [76]. Typical experimental model for this defect has been shown in Figure 15.

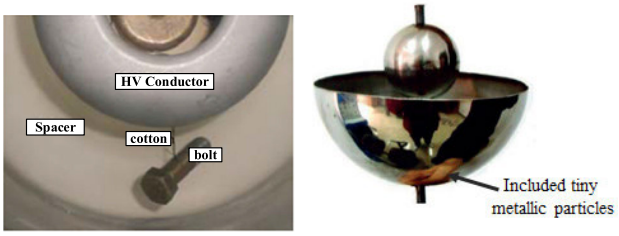

FIGURE 15. Experimental models used for free-moving particle [77], [78].

They can provide conductive local path and localized arcing which, in turn, would decrease the dielectric strength between high voltage conductor and outer enclosure. Factors like number of free particles, their size and shape, location (in vicinity of high/low field gradient) represent severity of PD pulses and their detectability [78]. The behavior of floating metals inside the GIS is similar to the corona discharge, in which case charges will accumulate at the sharp spots of the particle and PD would happen due to the electric field enhancement [79].

2) METALLIC PROTRUSION

This kind of defects formed during protruding parts like high voltage conductor generate high localized field around their sharp tips and most of time induce stable PDs even in applied rated voltage. Extreme electric field during overvoltage operation or fast transient overvoltage incidents can cause fast gas ionization. Some smaller defects can be harmless in the long-run and will be ablated unlike bigger particles [78]. Figure 16 shows typical models used for this defect.

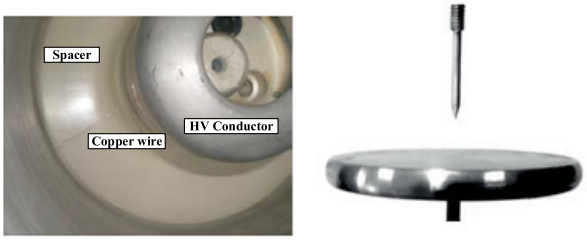

FIGURE 16. Experimental models used for metallic protrusion [77], [78].

This defect has been modeled in some studies based on Finite Difference Time Domain (FDTD) [79]. Impact

of the polarity on possibility of PD initiation has been described in [79].

3) GAP/VOID IN THE SPACER

This type of defect represents the internal bubbles of impurities of epoxy resin on the basin-type insulator formed during the manufacturing process or external due to chemical decomposition of gas in presence of discharges between loose connection of insulator and HV conductor. Internal defects will gradually deteriorate insulator and are difficult to detect. Also, mechanical vibration in a long-term operation would make loose connection between spacer and HV conductor in which local PDs can weaken insulation strength and result in major failure of gas-insulated equipment [76], [78]. Figure 17 shows commonly used models for this defect.

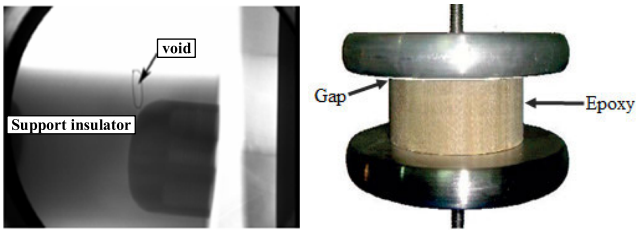

FIGURE 17. Experimental models used for gap or void in the spacer [77], [78].

4) INSULATOR CONTAMINATION

As mentioned before, floating metallic particles can be produced in different steps before or after erection of equipment. These free particles can move inside the gas insulation and sit over the insulator. Accumulation of charges over some of the fixed particles, or higher potential gradient across the particles due to mechanical vibration under electrostatic force can trigger localized surface discharges, which in turn would decompose high electronegative chemical components from surface and/or deteriorate insulator and/or cause surface tree and flashover on the surface of insulator [76], [78]. Typical experimental model for this defect has been shown in Figure 18.

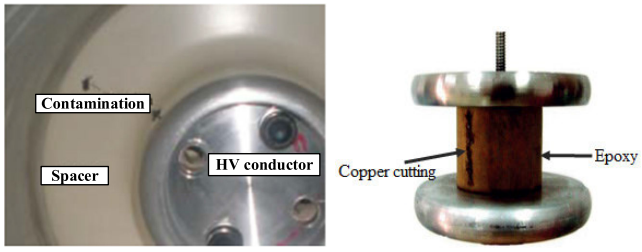

FIGURE 18. Experimental models used for metallic contamination defect on the insulator [77], [78].

5) GAS IMPURITY

Presence of any kind of gases especially water vapor mixed with main insulation (SF_6) can deteriorate the performance of insulation and will divert the uniform electric field and increase the possibility of PD occurrence in localized high electric field regions. Because of persistent discharges, recombination of impurities and SF_6 can produce more active and toxic components involved in faster degradation of insulation such as low-fluoride sulfide byproducts (SF_4, SF_3, SF_2, S_2F_{10}), and SO_2, SOF_2 and SO_2F_2 [80]–[82]. Generally, the dissolved-gas sensors are used to detect these impurities which is not the focus of this paper. Therefore, this type of defect is not presented in the next section.

Also, CIGRE working group D1.03 [75] has summarized the main features of different types of defects inside the GIS (given in Table 1) which shows the floating particles can have higher PD magnitude.

TABLE 1. Sensitivity of PD measurement for different defects inside the GIS [75].

Type of defect	Critical defect		Detectable length of defect at U_n [mm]
	Length [mm]	Apparent charge acc.to IEC 60270	
Moving particle	3 – 5	2 - 10 pC	3 - 5
Protrusion on HV conductor	around 1	1 - 2 pC	3 - 4
Protrusion on enclosure	4 – 6	2 pC	10 - 15
Particle on insulation	1 – 2	about 0.5 pC	3 - 10
Void	3-4 (dia)	1 - 2 pC	2 – 3

Overall, Since the replacement and maintenance time in gas-insulated equipment is relatively higher than other high voltage equipment, knowing the type of detected discharge signals is crucial in condition monitoring of these components. Risk assessment procedure is needed to decide whether the HV component can operate in normal condition without any possible failure or not. Severity of each defect should be evaluated based on reliable identification and evaluation technique. Risk of possible failure for different kind of defects and criticality range have been discussed in [87] and categorized accordingly in Figure 26.

III. PD PATTERN IDENTIFICATION

The PRPD patterns refer to a two-dimensional or three-dimensional pattern representation that describes the trajectory, frequency and phase relationship of PD signals over a period of time. These patterns represent cumulative PD information extracted for a specific time period and can include information about source, type, intensity of PDs. Extensive studies have already been carried out to introduce these patterns corresponding to different type of PD sources. Aim of this section is to summarize these research studies and discuss the main PD features which can indicate the occurrence of different PD types in different high voltage equipment.

A. HV MOTORS AND GENERATORS

PD testing has firstly been used as a method to determine the insulation condition of the stator windings of rotating electrical machines in the 1940s [88]–[90]. However, how to accurately identify the characteristics of different discharges from PD signals has become the key point in this field [91]–[93]. Stone proposed four separate separation methods for reducing the false identification of discharge pattern [94]. He believed that it is prudent to use separate algorithms for separating signals [95]. Contin showed that the PRPD recognition procedure based on shape analysis should be regulated to specific insulation techniques [96]. This section categorizes and analyzes five types of discharges recognized in high voltage motors and generators.

1) INTERNAL DEFECTS

The internal PD activity is characterized by the symmetry of the maximum amplitude and the number of discharge pulses which appeared in opposite polarities [97]. Hudon *et al.* conducted on-line monitoring of internal discharges on a 13.8kV generator. In addition, they used the stator winding of the generator for off-line testing in the laboratory. It was observed that the PD activity usually starts at several thousand volts below the nominal voltage [3], [98]. It can be seen in Figure 19 that PRPD results obtained in both offline and online measurements for internal discharge are almost the same. Their data show that the maximum amplitude of internal PD in off-line experiment is higher than that in on-line experiment. Normally, when the main insulation of the stator coil degrades, the amplitude of the internal discharge will decrease until it stabilizes at a lower constant level. This also proves that the minimum amplitude of internal discharge is allowed in a generator in service.

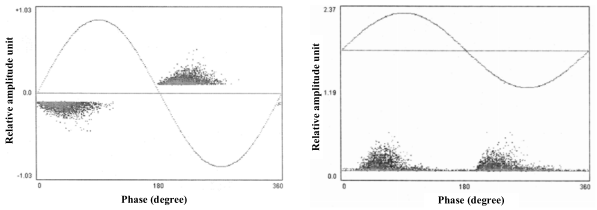

(a) (b)

FIGURE 19. PRPD pattern of internal discharge activity for a: (a) single stator coil (8kV) without artificial defect in the laboratory, (b) 30 MVA/13.8kV generator under operation [3].

Also, Kim *et al.* conducted offline and online experiments on the main insulation of seven 6kV motors in service [2], [99], [100]. Figure 20 shows another example of the PRPD pattern of internal discharge. The discharge amount and the discharge phase of the positive and negative half cycles are symmetrical.

Li *et al.* put a width-adjustable stator core slot model on the 10kV winding. First, they applied 6 kV voltage to the winding for 1 hour, and then recorded internal discharge PRPD pattern at 3-10 kV [5]. The measured PRPD fingerprint is

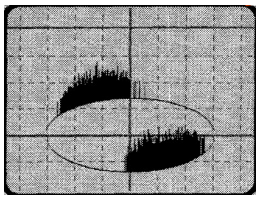

FIGURE 20. Internal discharge PRPD pattern from a large 6.6kV motor in off-line experiment [100].

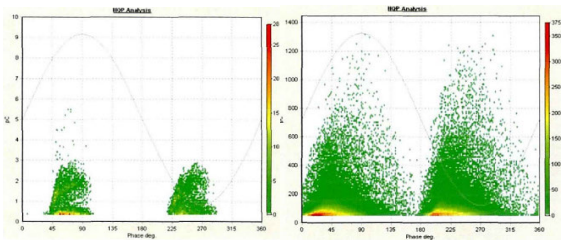

(a) 3kV (b) 10kV

FIGURE 21. PRPD pattern of internal discharge at different voltages tested off-line in a factory [5].

shown in Figure 21. The maximum magnitude of the internal discharge is within a certain voltage range, and increases with the applied voltage; however, the maximum value is not high and finally stabilizes at a level below 1500 pC. In addition, the discharge density increases as the voltage increases, and the discharge fingerprint moves to the left, but the PRPD fingerprint shape does not change.

2) SLOT DEFECTS

The PRPD pattern of slot discharge is quite different from the internal discharge. There is a significant asymmetry in the discharge count and discharge amplitude on the positive and negative half cycles. Because oxidation of the steel surface due to the PD repetition increases the availability of the electrons during the positive voltage half-cycle and leads a transition from a small number of PDs with large amplitude to a high repetition of smaller pulses [101]. In addition, a typical PRPD of slot discharge features a very steep slope at the beginning of the discharge pattern in the negative half cycle of the AC voltage in a form of triangular [102], same as the pattern in Figure 22. The part marked by the dotted line in the negative half cycle resembles a triangle mixed with noises.

Many parameters affect the mechanism of slot PD, such as temperature, humidity, gap size, mechanical vibration and insulation aging, which have been investigated by other researchers [104]–[106]. In addition, different types of stresses (such as electricity, heat, and mechanical) have an effect on discharge process, but more experiments are needed to distinguish the PRPD pattern changes of the slot discharge under different stresses [11], [12], [103].

a: PRPD VARIATION WITH VOLTAGES

Joyo *et al.* [17] made a 50mm diameter conical defect in the insulation of the stator bar of the 20kV generator, with a depth

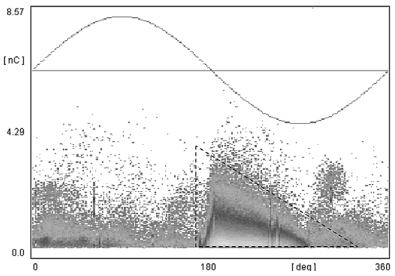

FIGURE 22. On-line PRPD pattern of slot discharge activity in a generator of 630 MW at 18 kV with mica-epoxy insulation, operated for 15 years [103].

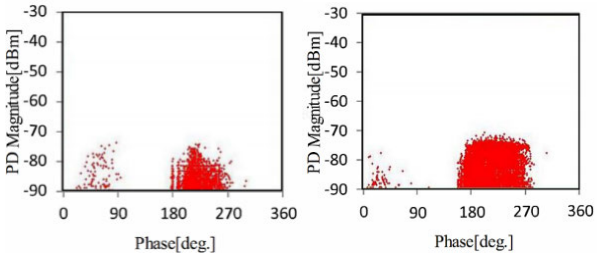

FIGURE 23. PRPD pattern of slot discharge measured at 10.5kV (left) and 18.5kV (right) using the experimental model shown in Figure 3(e) [17].

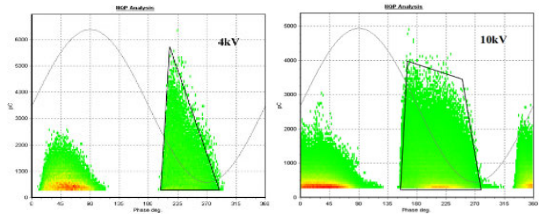

FIGURE 24. PRPD pattern of slot discharge measured at 4kV (left) and 10kV using the experiment platform shown in Figure 3(d) [13].

of about 76% of its thickness. The slot PD was measured at a voltage level of 10.5 kV and 18.5 kV at room temperature (Figure 23). Also, Song *et al.* [13] used a 10 kV motor stator bar with an insulation thickness of 2.03 mm and artificially reduced insulation layer thickness of 0.2mm [13]. The slot PD was measured at a voltage of 4 kV and 10kV at room temperature (Figure 24). They all found that the shape of PRPD pattern of slot discharge changes from a triangle to a quadrilateral as the voltage increases. At the same time, the change also occurs in the phase that PRPD pattern of the negative half cycle moves to the left.

b: PRPD VARIATION WITH AGING

Levesque *et al.* found that the aging of the insulating surface also affects the PRPD fingerprint. During aging, thermal effect on the surface increases the surface conductivity of the insulating material. As the insulating surface ages due to discharge, the number of discharges with higher magnitudes in the PRPD pattern decreases, and the number pulses with low amplitude increases [101]. Joyo *et al.* [17]

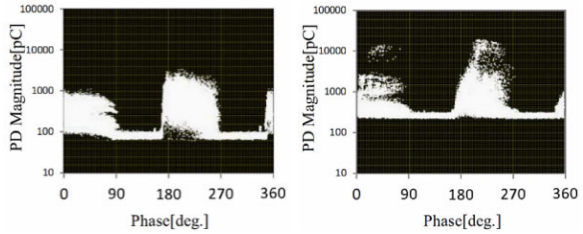

FIGURE 25. PRPD pattern of cone-shaped defect with different wearing level on the stator bar insulation at 12.1kV voltage (left 30%, right 76%) using the experimental model shown in Figure 3(e) [17].

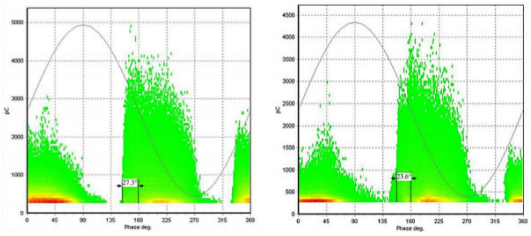

FIGURE 26. The phase shift of the slot PD pattern under different degrees of aging wear 0.2mm (left)and0.4mm (right) [13].

using the experimental platform shown in Figure 3(e), and Song *et al.* [13] using the platform given in Figure 3(c) showed the effect of insulation wear on PRPD pattern of the slot discharge. Their results show that the different wearing on the stator bar insulation might lead to different PRPD patterns (Figure 25). Also, It was found that the initial discharge phase of the positive and negative discharge pulses shifts to the left as the aging wear increases, and the phase shift decreases as the wear aging develops deeper (Figure 26).

c: PRPD PATTERN VARIATION WITH TEMPERATURE AND HUMIDITY

Some related studies show that temperature and humidity have certain effects on the slot discharge [108], [109]. Levesque *et al.* [106] using the experimental platform shown in Figure 3(b), studied the impact of temperature (at 28 °C and 85 °C) and different humidity levels (at 5, 9 and 13 g/m^3) on slot discharge pattern results. They found that the activity of slot discharge increases with temperature because the electron ionization effect in the gap is enhanced and the air density is reduced to generate more discharges as the thermal energy increases (Figure 27). In addition, the humidity in the air causes a general decrease in the activity of slot PD (Figure 28), mainly due to the electronegativity of the water molecules, which capture the free-moving electrons and suppress the development of discharge [111], [112].

d: PRPD VARIATION WITH VIBRATION

Other researchers have confirmed through experiments that the vibration will affect the slots PD results. Wu's experimental platform is given in Figure 3(a). He measured PD characteristics under the condition of 50Hz and 100Hz vibration at different voltages [113]. It is found that the PD pattern

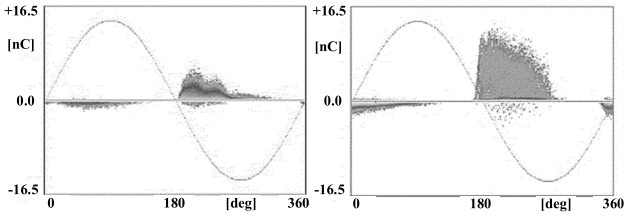

FIGURE 27. PRPD pattern of measured slot PDs at 8kV and 9 g/m3 before insulation aging (left 28°C, right 85°C) in a laboratory experiment [106].

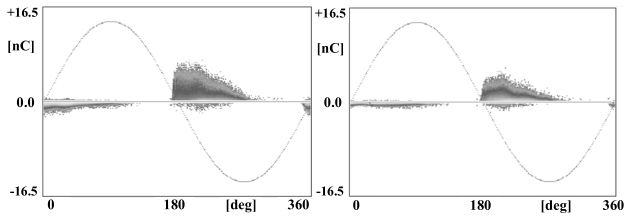

FIGURE 28. PRPD pattern of measured slot PDs at 8kV and 85°C after 230h insulation aging (left 9 g/m3, right 13g/m3) in a laboratory experiment [106].

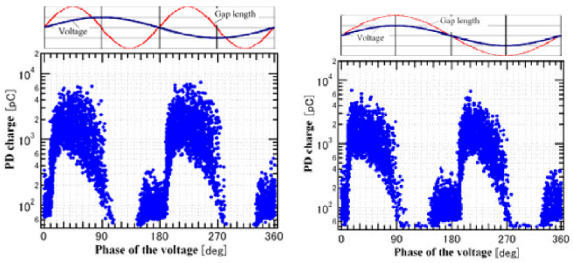

(a) 100Hz (b) 50Hz

FIGURE 29. PD patterns at two vibration frequencies and lead phase of 180 deg and the applied voltage is 6 kV [15], [113].

changed obviously with the frequency of vibration, and the PD magnitude is closely related to the gap length, while the larger PDs occur in a longer gap. When the frequency of vibration reaches a certain level, it will affect the PD activity. It can be seen in Figure 29 that the higher the vibration frequency, the larger the discharge amplitude and discharge density [15], [113].

3) DEFECT IN SLOT EXIT

The discharge amplitude of the corona discharge generated at the end of stator winding on the positive and negative half cycles is as asymmetric as the PRPD pattern of the slot discharge and both number and magnitude of positive discharges are greater than the negative discharge [114]. When the corona activity is strong, the asymmetry of the maximum amplitude tends to disappear whether the voltage is increased or the insulation is more deteriorated [3]. However, even if the PRPD patterns of the positive and negative half cycles are almost symmetrical, the number of positive and negative discharge pulses are not the same (Figure 30). Noting that the

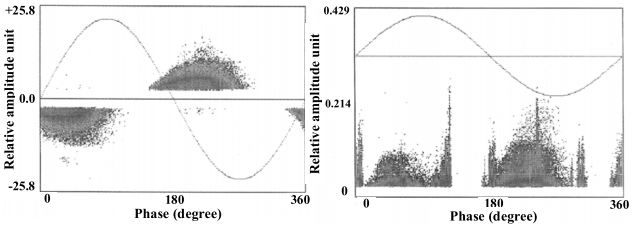

(a) (b)

FIGURE 30. (a) Corona discharge PRPD pattern measured in an off-line experiment at the junction of the 13.8kV stator winding coating, (b) corona discharge PRPD pattern on a 680 MVA/24 kV turbine generator with six exciter pulses during normal operation [3].

six vertical spikes with a 60° pitch in Figure 30(b) are not PDs but alternating phase of excitation current.

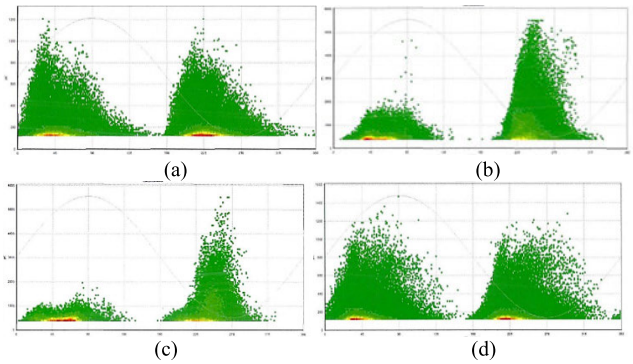

(a) (b) (c) (d)

FIGURE 31. PRPD pattern of: (a) acid environment and (b) neutral environment with relative humidity of 40% under 6kV; PRPD pattern of: (c) alkaline environment with relative humidity of 40% and (d) neutral environment with relative humidity of 60% under 6kV tested off-line in the factory [5].

Li *et al.* studied the effects of external conditions (humidity and acidity and alkalinity) on corona discharge. It was found that corona discharge did not occur in an acidic environment with a relative humidity of 40%, as shown in Figure 31(a). In a neutral or alkaline environment, it can be seen in Figure 31(b, c) that the discharge amount and the number of discharges of the negative half cycle are significantly larger than the positive half cycle, which is a typical PRPD pattern of corona discharge. Figure 31(b, d) shows the PD signal measured with a relative humidity of 40% and 60% in a neutral environment. It can be seen that the discharges of the positive and negative half cycles are similarly symmetrical, indicating that corona discharge does not occur. It was then concluded that the acid gas environment can effectively suppress the occurrence of corona discharge, and the higher the humidity ratio, the less likely corona discharge to occur [111]. Kang *et al.* studied the effect of relative temperature on corona discharge, where the effect of temperature on corona discharges was confirmed [16].

4) INTER-PHASE DEFECTS

Inter-phase PDs often occur at the ends of the two stator windings and may occur between bars of different phases

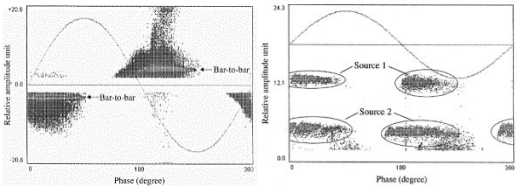

(a) (b)

FIGURE 32. (a) PRPD pattern of bar-to-bar discharge at 20kV measured in an off-line experiment, (b) PRPD pattern of bar-to-bar discharge measured on a 120 MVA /13.8 kV generator in an off-line experiment [3].

or between high-voltage bars and neutral bars of the same phase. There is an almost constant discharge amplitude on each of the positive and negative half cycles in PRPD pattern of bar-to-bar discharge. The number and amount of bar-to-bar discharge increase with increasing voltage. The negative discharge of the positive half-cycle is always higher than the positive discharge of the negative half-cycle and the negative discharge phase width is always narrower than the positive discharge phase width. However, it is relatively indistinguishable because it is often mixed with other PD signals [3], [107], [114]. Also, the PRPD pattern of bar-to-bar discharge is more obvious with the increase of voltage, but it can also be accompanied by the activity of corona discharge, as shown in Figure 32 reported by Hudon *et al.* Another example of bar-to-bar discharge measured on a running generator (120 MVA / 13.8 kV) is given in Figure 32(b). There are two bar-to-bar discharge sources in PRPD pattern, which are elongated shape and parallel to the coordinate axis., and the amplitude of the PD is relatively stable. In addition, bar-to-bar discharges may exist simultaneously with surface tracking.

Li *et al.* used the stator bars of a 10kV motor to conduct the bar-to-bar discharge experiments at 9kV and 15kV [5], [18]. They found that the bar-to-bar PRPD patterns will gradually move from the positive half cycle to the negative half cycle under power frequency voltage (Figure 33). This phenomenon is related to the movement of accumulated charge on the surface of the insulating medium.

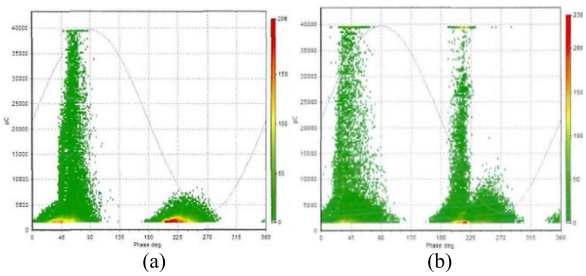

(a) (b)

FIGURE 33. (a) PRPD pattern of bar-to-bar discharge at 9kV on a l0kV HV motor, (b) PRPD pattern of bar-to-bar discharge at 15kV on a l0kV HV motor tested off-line in a factory [5].

Both the offline bar-to-bar discharge experiment conducted by Hudon and the online experiment by Li have vertically concentrated discharges in PRPD pattern. The reason for this phenomenon is mainly due to dust or other contamination on the insulating surface, which cause surface tracking.

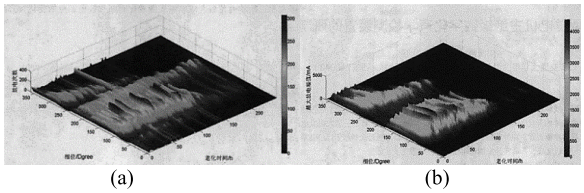

(a) (b)

FIGURE 34. (a) Aging time - phase - number of discharges; (b) Aging time - phase - maximum discharge amplitude tested in the laboratory [24].

5) SPARK EROSION

Vibrational sparking occurs anywhere in the slot winding [6]. H. You *et al.* studied the regularity of the PRPD pattern of spark discharge with insulation aging time. Figure 34 shows a three-dimensional spark discharge PRPD pattern. The spark discharge PRPD pattern is characterized by asymmetric pattern. The number of average discharge amplitude of positive half-cycle discharges are always higher than the negative half-cycle. Its main discharge energy is concentrated around 90° of the positive half-cycle and 270° of the negative half-cycle [24]. Spark discharge is more intense and more destructive than other discharges, causing serious insulation damage in a short period of time.

B. HV CABLES AND ACCESSORIES

Defect identification has been studied for several decades using PD patterns and features for power cables. Each type of PDs introduced in section 2.2 for this equipment has their own specific characteristics and PD features which can be used for cable condition assessment before any serious damage to insulation of cable and possible failure. Also, continuous monitoring of PD behavior can represent the degree of risk and intensity of PD progression in cable system. However, lack of knowledge about the location of PD source, insufficient sensitivity of measuring sensors to detect PD pulses with low magnitudes from small defects or aged defective cable insulation, as well as the presence of more than one PD sources make it difficult to determine PD source type, intensity, mutual impact of PD sources, and cable lifetime. In this section attributes of PD initiated by different PD sources have been summarized based on the well-known phase-resolved PD patterns.

1) METALLIC PROTRUSION IN AIR

discharges initiated by these protrusions can be initiated in all high voltage power electric components and have the similar PD pattern indication. They occur on the peak of the voltage and are detected on the negative half cycle of PD pattern when source of discharge is on the high voltage terminal. PD pattern is concentrated on the positive side when the source is on the ground side [27]. As mentioned before, this type of discharge does not threaten the cable insulation

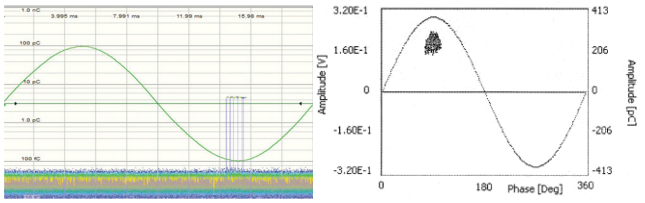

FIGURE 35. Corona discharge PD pattern in a laboratory experiment given in [27] (left) and [115] (right).

and accessory. However, inception voltage of this discharge generally is lower than other type of discharges and has to be recognized and segregated from the more harmful types of discharges. Figure 35 shows two different patterns identified as corona discharge.

2) SURFACE DEGRADATION

The surface defect is formed and intensified by high current density and higher discharge amplitudes in the range of 100 to 1000 pC and occurs after the zero crossing of applied voltage [27]. Unsymmetrical distribution of PDs in positive and negative half-cycles is commonly recorded PRPD pattern which depends on surface defect geometry and electric field magnitude and distribution (Table 2) [27], [116]–[118].

TABLE 2. Different types of geometries for surface discharge source.

1. Joint between cables (plot for 8.5kV, V_{inc}=5.5kV)		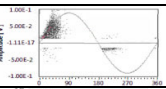	[118]
2. Edge to edge electrodes over the EPR film (8kV)	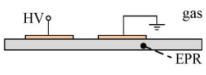	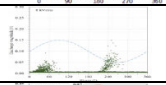	[119]
3. Rod to ring electrodes over the EPR film (4.1kV)	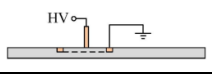	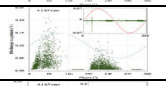	[119]
4. Needle to edge electrodes over the EPR film (4.1kV)	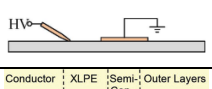	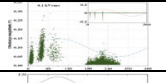	[119]
5. Ring-cut defect in the XLPE cable termination	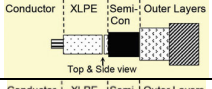	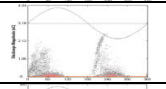	[120]
6. Trimline defect in the XLPE cable termination	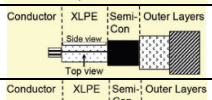	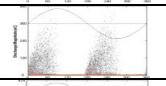	[120]
7. Semicon-feather defect in the XLPE cable termination	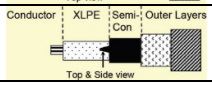	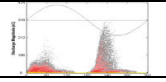	[120]

3) INTERNAL DEFECTS

Two major types of defects can be defined as the source of internal discharge: cavities and trees. Defects such as protrusion, contaminants can be the cause of electrical and water treeing inside the insulation due to intensifying the electric field in a local spot. Also, degraded wall of cavities in aged insulation can initiate electrical trees which can represent more complicated situation for discharge type identification.

a: CAVITIES

PD activity inside the cavities of an insulation depends on many parameters which can have significant impact on measured PD pulses and cumulative patterns. These parameters are insulation parameters (such as permittivity, conductivity, and temperature), geometrical parameters of the cavities (such as size, location, shape), internal void parameters (such as pressure, temperature, chemical compounds of enclosed gas), and applied voltage source parameters (such as amplitude, frequency, waveform). Aging and continuation of PD can dramatically affect internal parameters as well as the shape and size of the void overtime. These parameters have been explained in [31], [32] using the proposed model and discussed and compared with experimental results presented in other research works.

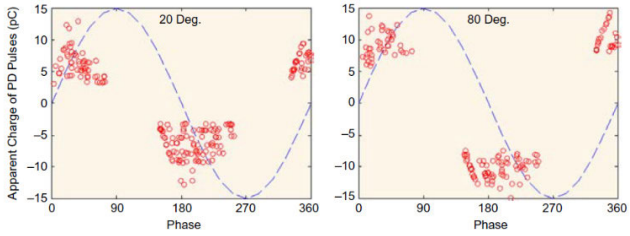

FIGURE 36. Temperature impact on PRPD pattern for 1mm dielectric bounded obtained from the simulation model [116].

Temperature of insulation can affect thermal extension factor, conductivity and permittivity of insulation, gas pressure inside the void and breakdown voltage, probability of PD occurrence and residual voltage which have been considered in proposed 3-capacitors model [32]. Figure 36 shows that the rise of the temperature can expand the pattern in both cycles and decrease the repetition rate which have been verified by experimental results in [119].

Also, higher average of PD apparent charge and number of PD pulses for the cavities close to high voltage conductor are implied by Figure 37.

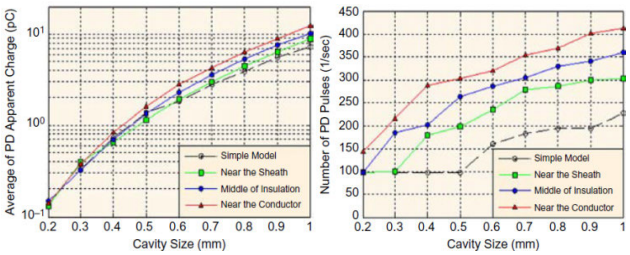

FIGURE 37. Influence of cavity size and location on average PD charge and number of PDs obtained from the simulation model [32].

Different types of PD patterns can be observed for a cavity overtime due to physical and chemical changes inside the void arising from degradation process. Increase of surface conductivity, gas dissociation inside the void and production of electronegative gases, pressure and humidity variation, chemical reactions on the surface will happen during

TABLE 3. Pattern trends during aging process.

Stage 1	Stage 2	Stage 3	
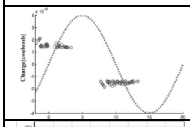	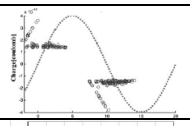	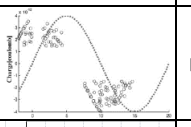	[31]
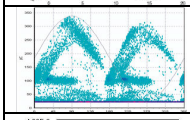	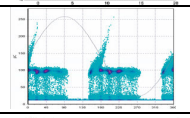	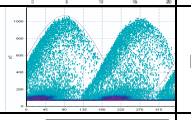	[33]
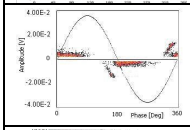	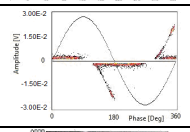	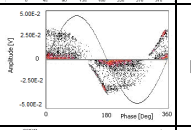	[122]
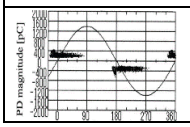	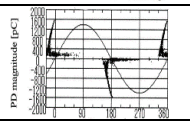	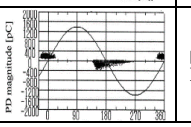	[123]

the aging process [120]–[122]. Pattern transformation from turtle-like to rabbit-ear like and then to bulgy have been defined and simulated based on physical and chemical changes in [31]. Similar results for these three stages have been reported in different research works as shown in Table 3.

b: ELECTRICAL AND WATER TREES

As discussed in section 2.2.3, ETs and WTs are ignited by overvoltage and initial conductive branch can provide enough free electrons around the tips to generate PDs. Although physical and chemical processes during treeing phenomenon have not been thoroughly understood, condition of insulation and vulnerability to internal trees can be evaluated by detecting the PD pulses.

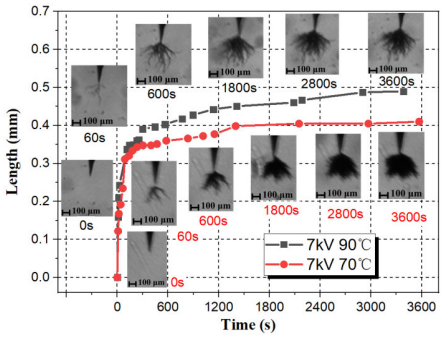

FIGURE 38. Electrical tree development over test time at 70°C and 90°C tested on the laboratory model [123].

Zhu *et al.* have presented ET growth inside the XLPE at 70°C and 90°C for one hour which shows rapid growth in first minute of the test and then continuous increase with lower rate [123]. Also, tree length at higher insulation temperature is higher as shown in Figure 38.

Extracted PRPD patterns during the test for 20 seconds shows that PD magnitude remains constant for last two

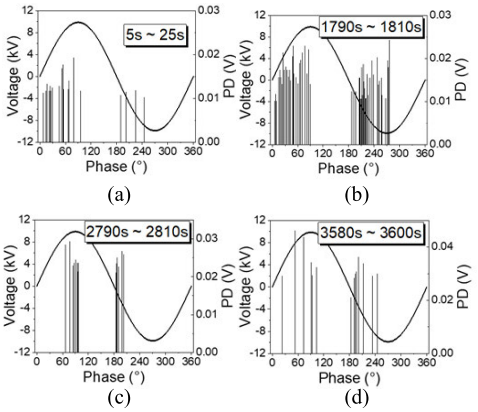

FIGURE 39. PRPD pattern during ET growth at 90°C [123].

recorded data sets (2800s and 3600s). PD number increases until the 1800s and then starts to decrease (Figure 39).

Chen *et al.* have investigated PD behavior of two main types of ETs, i.e. branch-like and bush-like trees, by tracking the main PD parameters (maximum magnitude of apparent charge, Q_{max}, pulse repetition, N, and the discharge power, P) in XLPE insulation using the embedded needle electrode at different voltage levels [34], as shown in Figure 40. They have illustrated how more densely packed structure is formed at higher voltages.

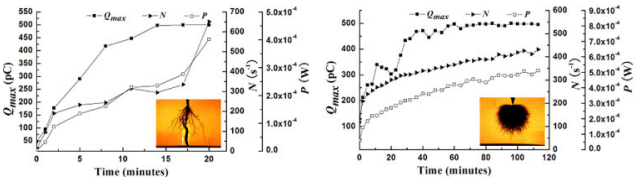

FIGURE 40. PD characteristics of branch like tree at 11kV (left), and bush-like tree at 15kV from the laboratory experiments (right) [34].

Du *et al.* have examined influence of temperature of HV and ground electrode as well as temperature gradient on the development of ETs and PD characteristics [124]. As shown in Figure 41, by increasing the temperature gradient, PD magnitude increases, while at higher temperature of HV electrode, PDs with lower magnitude are observed.

C. HV TRANSFORMERS

The PD pulse amplitude and its phase position are the most commonly measured parameters to use in PD as diagnostic techniques for transformers. The PD pulse amplitude is used as an index to the quality of the insulation under test whereas the phase information is used to identify the type of PD [46], [125], [126]. The waveform characteristics can be used as the basis for distinguishing types of discharge source [46]. Statistical analysis techniques sometimes are employed to monitor the changes of the PD features (e.g. the PD pulse magnitude, repetition rate, and power spectrum) in 2-D models. Focus of this section is to present the main

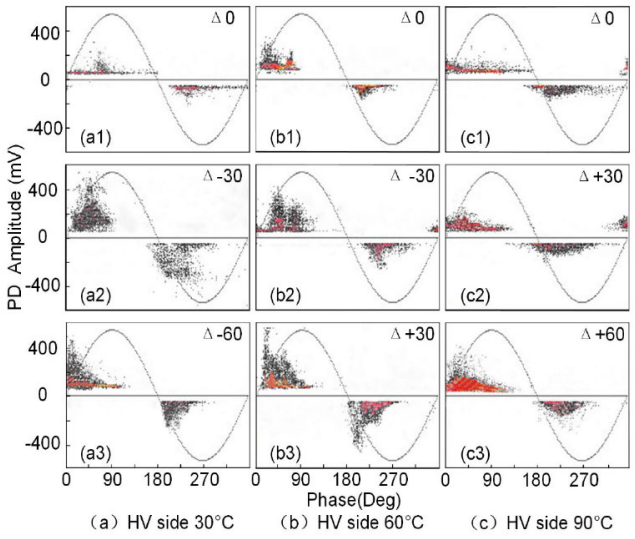

FIGURE 41. PRPD patterns at different HV electrode temperature and temperature gradients at 5 min obtained from an experimental model.

features of PRPD patterns in order to identify the PD source and severity of the defect.

1) METALLIC PROTRUSION

Previous studies regarding this type of defect indicate that a smaller number of PDs are detected as pressure or temperature of oil increases, while moisture has the opposite impact on the number of PDs. Also, PD number decreases when the oil ages which makes the insulation condition assessment much more difficult [51]. In [43], [52], [127], the impact of viscosity and oil type on the PD count and charge have been investigated. Negative and positive corona have different inception voltage and PD characteristics such as the number and magnitude of PDs. Figure 42 shows two PRPD patterns for needle-plane configuration embedded inside two different types of oils recorded by other research groups.

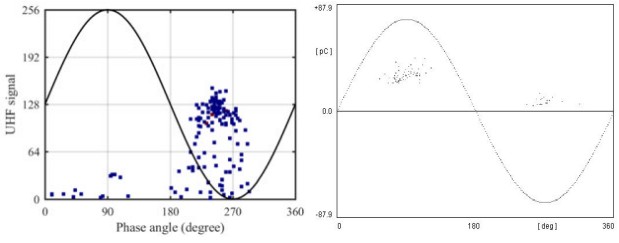

FIGURE 42. protruding defect consist of isosceles triangle copper plate and insulating plate layer in the oil [43] (left), needle-plane configuration embedded in NYTRO 10XN oil [52] (right).

Impact of oil temperature and humidity on PD inception voltage for specific needle-plane configuration inside the oil given in [52] is shown in Figure 43.

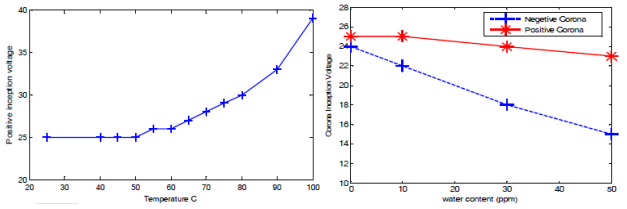

FIGURE 43. PD inception voltage versus: temperature (left), humidity (right) using an experimental model [47].

2) CAVITIES

This defect is identified by the clouds of PD pulses which sweep upward forming arcs on the phase-resolved plot. This pattern indicates distributed gas voids in the oil-paper insulation [128], [129]. In addition, the discharges only on one-half cycle are usually attributed to the external sources. When the PD pattern on the positive-half cycle is a mirror image of the negative-half cycle of the applied voltage, it is called symmetrical. This can be a reason that the dielectric materials at either side of the defect generating discharge are the same, or similar. Therefore, there is a high possibility that PDs are happening at a void in the oil-paper insulation. On the other hand, the PD pattern would probably be different on the positive and negative-half cycles if the materials at either side of the defect differ [128].

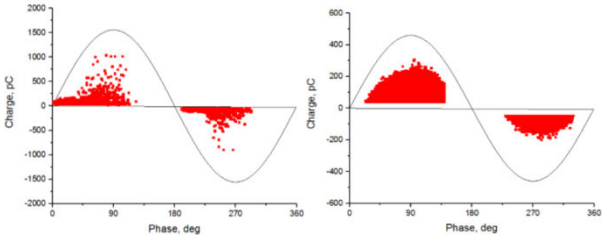

FIGURE 44. PRPD patterns of internal PDs tested in the laboratory for (left): new pressboard and (right): aged oil impregnated pressboard of power transformer [54].

The results from the PD measurement show that the influence of relative humidity on Kraft paper. The PD magnitude of aged pressboard drops to the lower value compared to the new pressboard (see Figure 44), which can indicate the effect of conductivity on the discharge mechanism [54], [130].

In Figure 45, the effect of different air gaps as well as oil moisture level on PRPD patterns of the oil impregnated papers are shown. The PD patterns for different level of moisture contents indicate similar trend in phase of occurrence of PD event with respect to the applied power frequency voltage [59].

3) SURFACE DIGRADATION

The creepage discharge on the surface of pressboard (PB) is usually more evident at smaller phase angles and the promotion of negative discharges would be more than positive ones [44], [131]. It is noteworthy to mention that because of the hydrostatic pressure influence on the surface discharge of

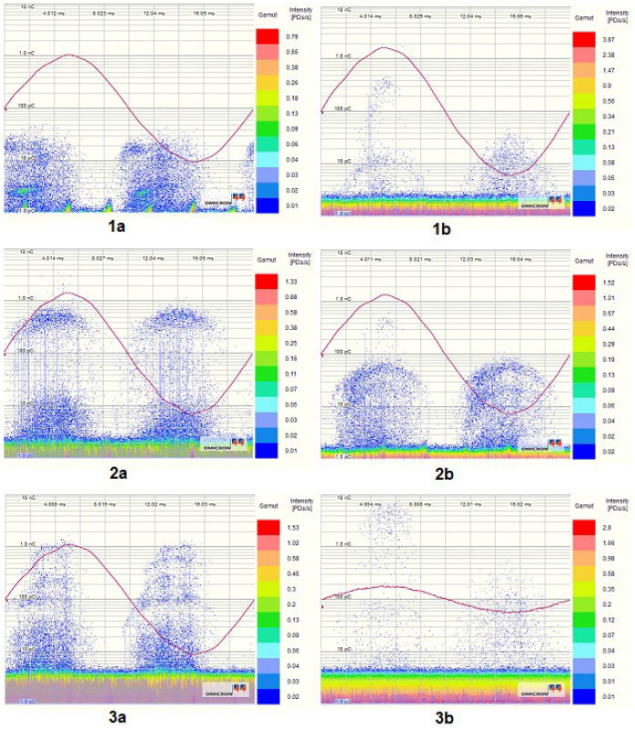

FIGURE 45. Typical PD pattern in OIP obtained in the laboratory, a: zero gap (between needle and pressboard laid on the ground electrode), b: 10mm gap. 1, 2 and 3 are 3.7%, 4.3% & >5% moisture content respectively [59].

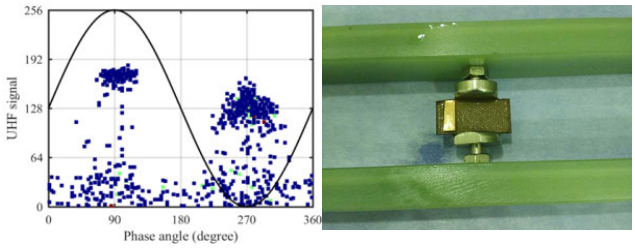

FIGURE 46. Surface discharge PRPD pattern (left) and experimental model (right) using a cardboard along the electric field direction and a copper sheet with the edge of the plate [43] .

oil-paper insulation, its characteristic can be different in high altitude from other places. Additionally, it has been shown that increase of hydrostatic pressure can reduce the PD charge amplitude to a very low value under normal operating conditions; on the other hand, it can result in significant increase of the maximum PD charge amplitude whereas the local electric field is overbalanced due to arising defect, so that PD identification would be easier in this case. In addition, the PD repetition rate decreases considerably when the hydrostatic pressure is increased. Thus, it can be useful to protect the oil-paper interface under a normal operating condition of HV transformers [44]. Figure 46 shows an experimental model to generate creepage discharge over the cardboard sample between the electrodes and corresponding PRPD pattern.

Yi and Wang have conducted a research on creepage discharge evolution over the impregnated pressboard by recording the surface tracking, PRPD patterns and discharge current signals. Different kinds of insulating liquids, synthetic ester MIDEL 7131, natural ester FR3 and mineral oil Nytro Gemini X, were used in their experiment [69]. They obtained and explained different stages in the process of surface tracking. Figure 47 shows the evolution of PRPD pattern at difference stages of creepage discharge on the pressboard in MIDEL 7131.

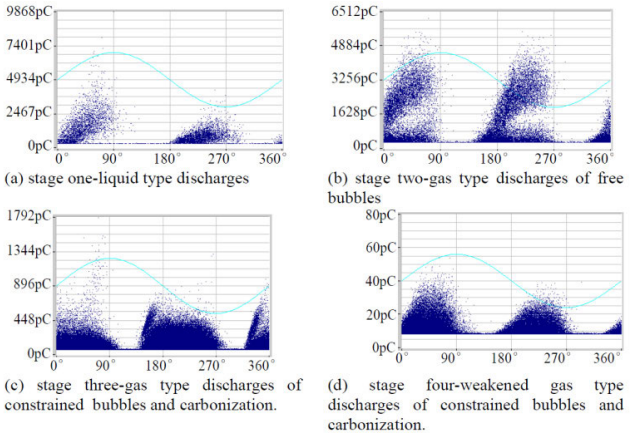

FIGURE 47. Evolution of PRPD pattern at different stages of surface tracking recorded at 43kV using an experimental needle-pressboard-ground model [69].

D. GAS INSULATED EQUIPMENT

Different types of PD sensors has been introduced and employed in gas-insulated equipment in order to have higher detection accuracy of assorted type of PDs, because repair or replace each compartment of this equipment are time-consuming, and highly reliable preventive measures are critical. Aim of this section is to illustrate the key features of PRPD patterns measured by these sensors from different PD sources inside the gas-insulated equipment.

1) FREE-MOVING METALLIC PARTICLES

Metallic particles can freely move inside the compartment of the GIS and/or lift off toward the HV conductor. Since their movement depends on particles size, weight and electrostatic force, PD pattern should be evaluated at different stages (e.g. Figure 48). PD pattern of measured signal can discriminate between moving and jumping stages at different applied voltages [132]. When electric field inside the enclosure is higher enough to overcome gravity force and weight of particles, they will jump from enclosure toward the HV conductor which intensifies discharges around the conductor. During this transition from jumping to the dancing mode, PRPD pattern does not show any clear changes and are not stable; also, PDs are distributed around zero crossing which goes toward the first half of positive and negative cycle of voltage in PRPD pattern and forms more symmetrical pattern (Figure 49). When metallic particles approach and attach HV conductor, PDs ignite with higher intensity at the

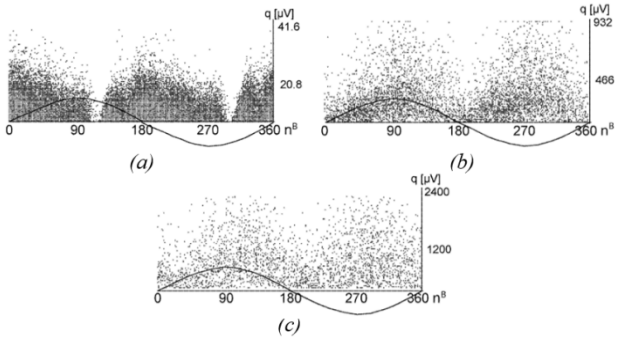

FIGURE 48. Extracted patterns for different conditions of 15mm free-moving particles using UHF couplers on the GIS on site: (a) shuffling, (b) dancing, (c) jumping [86].

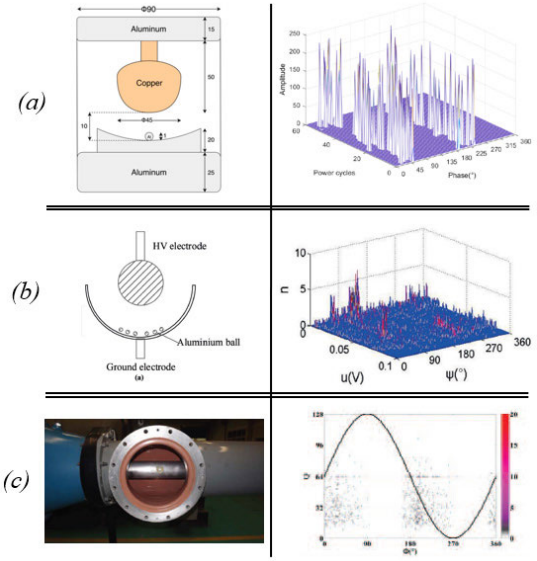

FIGURE 49. Flouting particle model and corresponding PRPD: (a) sphere diameter 1mm (10kV HV electrode) and concave ground electrode [134], (b) HV ball electrode with 44mm diameter and half hollow sphere ground electrode 120mm [78], (c) flat metal washer with the diameter of 33mm suspended by insulation tape in real 220kV GIS [135].

positive and negative half cycles and reach to the stable and symmetrical condition around the peak of voltage waveform (shuffling) [86], [133].

Also, Ju Tang et. al. has presented PD development trend for this defect as shown in Figure 50.

2) METALLIC PROTRUSION

In this kind of defect, due to space charge accumulation around the tip of protrusion and non-uniform electric field, negative corona discharges are detected around 270° in PRPD pattern for protrusion on the HV conductor. If the voltage is gradually increased, PDs in positive polarity are incepted with higher magnitude around 90° and intensity for both polarities with respect to other defects. Secondary electron emission plays major role in consistent occurrence of negative

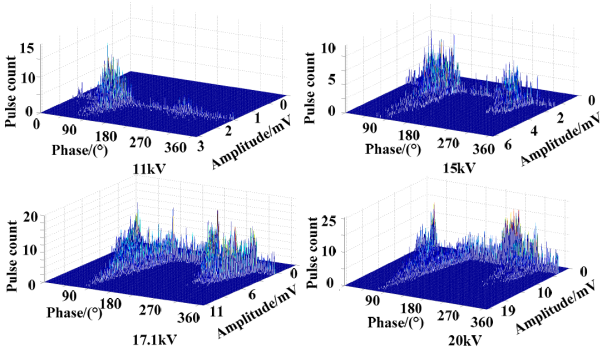

FIGURE 50. Change of the PD pattern with voltage rising for floating particles inside a simulated GIS in the laboratory [136].

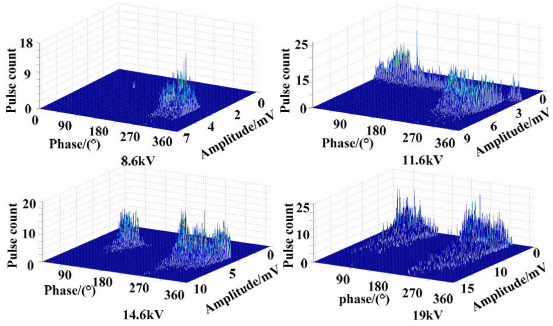

FIGURE 51. Change in PRPD pattern for different voltages above inception voltage for metallic protrusion defect [133].

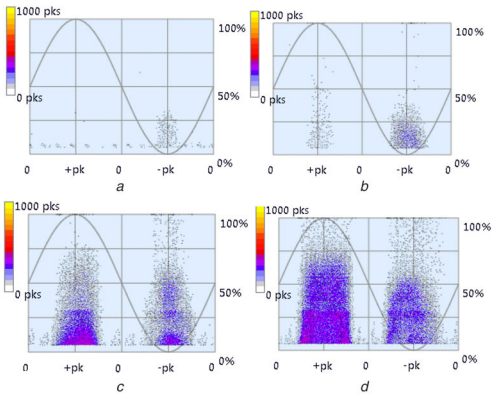

FIGURE 52. PRPD patterns for metal protrusion model on HV conductor inside a simulated GIS in the laboratory [136].

corona discharge. Positive charges accumulated around cathode enhance local electric field and cause higher number of electron avalanches at the same time [133]. Xian-Jun Shao in [133] and Ju Tang in [136] have shown progression of patterns for this defect with voltage rising as shown in Figures 51 and 52.

The tip shape of protrusion has significant impact on PD development process. For round shape, PD inception voltage and breakdown voltage are closer and late detection can lead fast failure in system; however, in sharp protrusion, depending on length of defect, more stable PDs can be

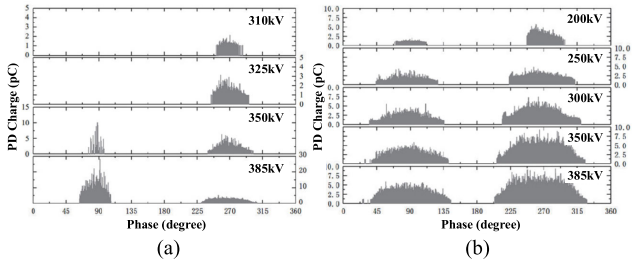

FIGURE 53. PRPD pattern for different applied voltages and protrusion defect sizes with a length of 6mm and radius of: (a) 0.5mm, (b) 0.25mm inside an experimental 550kV GIS chamber [137].

recognized earlier because the inception and breakdown voltage are noticeably different. No direct correlation between PD magnitude and defect length has been reported [75]. The protrusion shape factor has been discussed in another research work. Results show that, for a tip with small curvature radius, local electric field and its gradient is higher, which results in local PDs at lower voltages [137]. As shown in Figure 53, for sharper protrusion, positive and negative PD patterns are observed at lower voltages with higher magnitude and intensity for negative half-cycle.

3) GAP/VOID IN THE SPACER

PDs generated in the gap between the spacer and the metal conductor are not stable and have been distributed at the second half partition of positive and negative half-cycles. PD repetition rate and magnitude range are higher but average magnitude of discharges are much lower. Space charges are accumulated in the vicinity of insulator which causes electric field distortion in the air gap [78]. Maximum electric field is concentrated in the gap and inception voltage mainly depends on gap size, insulator property and applied voltage.

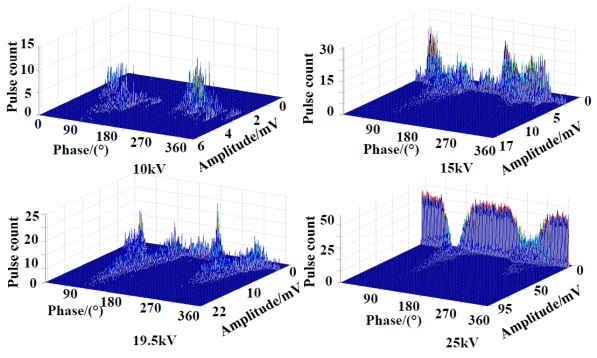

FIGURE 54. Change of the PD pattern with voltage rise for electrode gap defect [136].

That PRPD pattern changes with respect to voltage level higher than inception voltage has been given in [136] for electrode gap defect as shown in Figure 54. These results confirmed abovementioned explanations about PD magnitudes and repetition rates reported by other works.

Since magnitude of discharges for internal voids inside the insulator are much smaller, they might not be that dangerous for many years and will gradually deteriorate insulator during the aging process. Therefore, insulator void is assumed as medium risk defect in gas-insulated equipment unlike the protrusion which shows higher risk of failure [138]. Also, ''rabbit ear'' 2D pattern distribution as a signature of internal void has been reported in some works. When voltage increases, total internal electric field in the void during polarity reversal increases which in turn, results in higher magnitude of ear formed for each half-cycle as shown in Figure 55 [139].

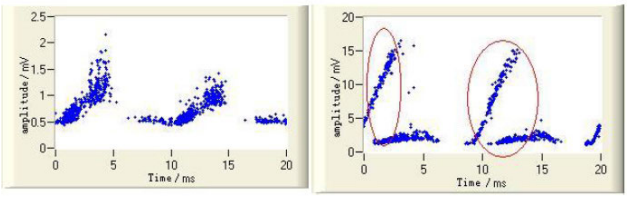

FIGURE 55. PRPD pattern at inception voltage (left), and higher voltage level (right) [136].

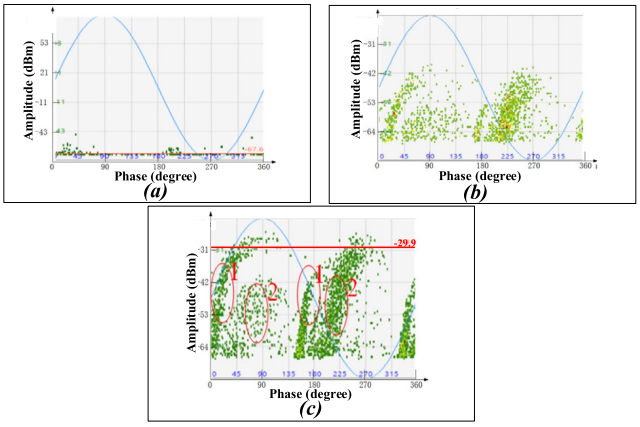

FIGURE 56. PRPD pattern results of on-site tests from a 550kV GIS insulating spacer with multiple internal voids at different voltage levels: (a) 220kV (inception voltage), (b) 382kV, and (c) 740kV [139].

Also, multi-ear PRPD pattern has been shown in [140] for extracted UHF signals of an insulating spacer having multiple internal voids at higher voltage levels above inception voltage as shown in Figure 56.

4) INSULATOR CONTAMINATION

For an insulator contaminated mainly by metallic particles, PD pulses would generate electrical branches on the spacer surface in which these surface discharges would have significant degradation consequences on the insulator. This type of PD is not stable and PRPD pattern shows lower repetition rate with relatively high average amplitude. Moreover, PDs are concentrated around peak of voltage waveform with a lower distribution toward second and fourth quadrants of the phase angle of the applied voltage [78]. PD patterns presented in different works show relatively symmetrical distribution for

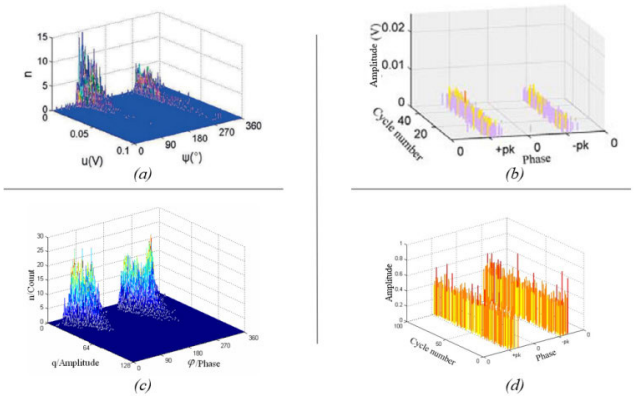

FIGURE 57. Typical PRPD patterns for contaminated insulator from the experimental models reported in: (a) [78], (b) [77], (c) [140], and (d) [141].

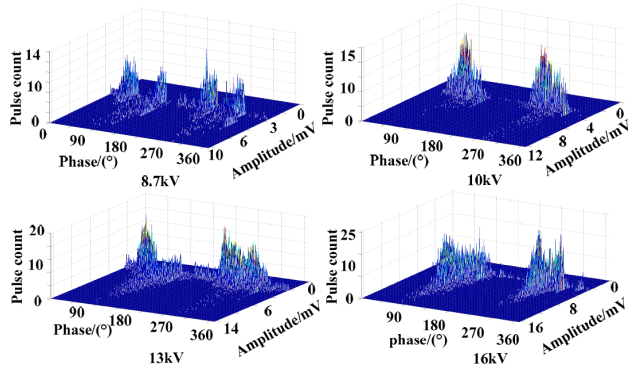

FIGURE 58. Change of the PD pattern with voltage rise for insulator contamination defect from the experiments given in [136].

positive and negative half-cycles in this defect (Figure 57). Also, Ju Tang in [136] has depicted pattern changes with voltage rise as shown in Figure 58.

IV. CONCLUSION AND OUTLOOK

A. SUMMARY

The high voltage PD measurement is one of the powerful diagnostic methods for insulation systems of different high voltage equipment. Comprehensive studies have been conducted on assessing the operating condition of high voltage equipment based on detected and measured PD data from defects as the PD sources in order to take every precaution to avoid the failure. We think that advances in PD data acquisition sensors have provided a great understanding of the existence and severity of different defects based on PRPD patterns which can be abridged, and the key features, signatures, similarities, and differences to be summarized and discussed. Summarized information can not only facilitate the engineering decision-making process before involving in sophisticated data analysis techniques but also highlight the main needs of further feature extraction and post-processing of available data in order to obtain further information as much as possible. Having this thought in mind, we have categorized and introduced commonly observed defects in high voltage equipment and their effects on normal operation and lifetime of these key components in section 2. Then, we have presented a summary of PRPD results reported by the researchers for each type of defect. In order to verify the consistency of the results, obtained PD pattern results by experimental models and on-site measurements have been given and illustrated in section 3. Also, the main features of these patterns for different types of defects categorized in this section have been summarized in TABLE 4.

B. OUTLOOK

Previous studies on PD patterns arising from the different PD sources in each high voltage equipment as well as the effect of different parameters such as pressure, temperature, humidity, location, geometry of defect provide reasonably good consistency of the PD characteristics. The significant impact of aging at each stage on PD patterns has been reported for specific types of defects which are subjected to physical and chemical changes over time. Important to note that the novel feature extraction and classification techniques have been adopted in the last decade and provide further information about the PD source and type which have not been introduced and discussed in this review. Despite the available knowledge and techniques for condition assessment of electrical equipment based on PD data, the following issues need to be considered in the future works:

- The presence of multi-PD sources as a highly possible case should be further studied. Identification of PD sources and separation of the patterns have not been successfully done using the available techniques. Sources with lower intensity due to less sensitivity of the sensors or attenuation of signals detected far from the PD source location cannot be detected and/or identified in this case.
- Utilizing sensors with high sensitivity is not always the best option, especially for on-site measurements. Environmental noises or unwanted signals and pulses from the grid can easily pollute the PD pulses, especially for PDs with low intensity due to the nature of the source. Robust denoising techniques are needed.
- The location of the PD source is not known in the real measurements. Multiple PD sensors are usually used to locate the sources, especially in cables and gas-insulated equipment. Although strategies and different implementations have been suggested to this end, their accuracy and efficiency have been confined to the specific system and arrangement.
- In some equipment, different types of sensors are used for condition assessment (e.g. gas-insulated equipment). A central decision-making technique needs to be established to correlate the data received from different types of sensors.
- One of the main reasons for extracting the PD data is for life expectancy. Although PD patterns can provide somehow the condition and aging stage of the insulation system, they cannot determine the life-time of a power component without continuously monitoring the PD behavior and extracted patterns.

TABLE 4. Summarized major features and signatures of PRPD patterns obtained for different types of defects observed in each high voltage equipment (HC: half cycle).

High Voltage equipment	Type of Defect	PRPD Pattern Signature
Motors and generators	Internal	Symmetry of the maximum amplitude and number of PDs in both HCs
	Slot	Asymmetric; higher negative half pattern with a possible shape of triangle or quadrilateral
	Slot exit	Asymmetry in the pattern peak magnitude or number of PDs detected for both HCs (higher possibility of higher PD magnitudes in negative half cycle)
	Inter-phase	Higher magnitude and narrower pattern for negative HC, possibly mixed with other PD source patterns like corona at higher voltages
	Spark erosion	Asymmetric pattern; more intense PDs for this defect than others; concentrated around the voltage peaks with higher magnitude in positive HC
Cables and Accessories	Metallic protrusion	Pattern forms in one of HCs
	Surface degradation	Unsymmetric patterns formed after the zero crossing of voltage; strong dependency on the defect geometry on the surface
	Internal (cavities)	Relatively symmetric for both HCs; turtle- or rabbit-like patterns depending on the aging stage
	Internal (trees)	Asymmetric patterns in terms of the shape, intensity or peak
Transformers	Metallic protrusion	Pattern forms in one HC, or significant higher PDs in one of HCs
	Cavities	Generally, symmetric patterns are formed in HCs
	Surface degradation	Asymmetry in each HC unlike the patterns described to cavities
Gas-insulated equipment	Free-moving metallic particles	Unstable pattern; generally symmetric with a peak between zero crossing of the voltage to the peak of voltage in each HC
	Metallic protrusion	Concentration of PDs with higher magnitude at the voltage peaks; starting from negative HC at 270º and then initiated at positive peak at 90º
	Gap/void in the spacer	Patterns for both HCs formed generally at the second and fourth quadrants
	Insulator contamination	Unstable patterns with low repetition rate and possible high average amplitude, concentrated around peaks toward the second and fourth quadrants

REFERENCES

[1] E. Gulski, "Digital analysis of partial discharges," *IEEE Trans. Dielectr. Electr. Insul.*, vol. 2, no. 5, pp. 822–837, Oct. 1995.
[2] H.-D. Kim, "Analysis of partial discharge to high voltage motor stator windings," in *Proc. Annu. Rep. Conf. Electr. Insul. Dielectric Phenomena (CEIDP)*, 2001, pp. 340–343.
[3] C. Hudon and M. Belec, "Partial discharge signal interpretation for generator diagnostics," *IEEE Trans. Dielectr. Electr. Insul.*, vol. 12, no. 2, pp. 297–319, Apr. 2005.
[4] S. Bin Lee, T.-J. Kang, H. Kim, T. Kong, and C. Lim, "Case studies of stator winding turn insulation failures in medium voltage motors," in *Proc. Annu. Pulp, Paper Forest Industries Tech. Conf. (PPFIC)*, Jun. 2017, pp. 1–8.
[5] C. Li, "Research on establishment method of partial discharge fingerprint database and discharge pattern recognition technology of high voltage motor stator winding," M.S. thesis, Dept. Elect. Power Eng., Taiyuan Univ. Technol., Beijing, China, 2014.
[6] G. C. Stone, C. V. Maughan, D. Nelson, and R. P. Schultz, "Impact of slot discharges and vibration sparking on stator winding life in large generators," *IEEE Elect. Insul. Mag.*, vol. 24, no. 5, pp. 14–21, Sep. 2008.
[7] M. Belec, C. Hudon, and C. Guddemi, "Laboratory study of slot discharge characteristic PRPD patterns," in *Proc. Electr. Insul. Conf. Electr. Manuf. Coil Winding Conf.*, 2001, pp. 547–550.
[8] G. C. Stone, H. G. Sedding, and C. Chan, "Experience with online partial-discharge measurement in high-voltage inverter-fed motors," *IEEE Trans. Ind. Appl.*, vol. 54, no. 1, pp. 866–872, Jan. 2018.
[9] M. Levesque, E. David, C. Hudon, and M. Belec, "Effect of surface degradation on slot partial discharge activity," *IEEE Trans. Dielectr. Electr. Insul.*, vol. 17, no. 5, pp. 1428–1440, Oct. 2010.
[10] M. Lévesque, C. Hudon, M. Belec, and E. David, "Evolution of slot partial discharges under electrical, thermal and mechanical stresses," in *Proc. IEEE Int. Sympos. Electr. Insul.*, 2008, pp. 153–157.
[11] M. Levesque, C. Hudon, M. Belec, and E. David, "Measurements of slot partial discharges with an antenna during accelerated aging," in *Proc. IEEE Electr. Insul. Conf.*, May 2009, pp. 458–462.
[12] C. Hudon, M. Belec, and M. Lévesque, "Study of slot partial discharges in air-cooled generators," *IEEE Trans. Dielectr. Electr. Insul.*, vol. 15, no. 6, pp. 1675–1690, Dec. 2008.
[13] J. Song, C. Li, L. Lin, Z. Lei, X. Bi, and H. Yang, "Slot discharge pattern of 10 kV induction motor stator coils under condition of insulation degradation," *IEEE Trans. Dielectr. Electr. Insul.*, vol. 20, no. 6, pp. 2091–2098, Dec. 2013.
[14] G. C. Stone and R. Wu, "Examples of stator winding insulation deterioration in new generators," in *Proc. IEEE 9th Int. Conf. Properties Appl. Dielectric Mater.*, Jul. 2009, pp. 180–185.
[15] K. Wu, M. Kanegami, T. Takahashi, H. Suzuki, T. Ito, T. Okamoto, and H. Yano, "Effect of mechanical vibration on the behavior of partial discharges in generator windings," *IEEE Trans. Dielectr. Electr. Insul.*, vol. 13, no. 2, pp. 345–352, Apr. 2006.
[16] A. Kang, M. Tian, C. Li, J. Song, S. Vincenzo Suraci, W. Li, L. Lin, Z. Lei, and D. Fabiani, "Development and pattern identification of end-winding discharge under effect of relative humidity and temperature for HV motors," *High Voltage*, vol. 5, no. 4, pp. 434–443, Aug. 2020, doi: 10.1049/hve.2019.0124.
[17] T. Joyo, T. Okuda, N. Kadota, R. Miyatake, S. Okada, and K. Mio, "Phase resolved partial discharge patterns for various damage of winding insulation detected with different measuring devices," in *Proc. IEEE Electr. Insul. Conf. (EIC)*, Jun. 2017, pp. 344–347.
[18] C. Li, J. Song, A. Kang, L. Lin, W. Su, and Z. Lei, "PD patterns of stator windings by in-factory experiment on a 10kV motor," in *Proc. Int. Symp. Electr. Insulating Mater.*, Jun. 2014, pp. 168–171.
[19] G. C. Stone, M. Sasic, D. Dunn, and I. Culbert, "Motor and generator windings," *IEEE Ind. Appl. Mag.*, vol. 17, no. 6, pp. 29–36, Nov. 2011.
[20] A. J. M. Pemen, P. C. T. van der Laan, and W. de Leeuw, "Analysis and localization of spurious partial discharge activity in generator units," in *Proc. IEEE 7th Int. Conf. Solid Dielectr. (ICSD)*, Jun. 2001, pp. 489–492.
[21] M. Liese and M. Brown, "Design-dependent slot discharge and vibration sparking on high voltage windings," *IEEE Trans. Dielectr. Electr. Insul.*, vol. 15, no. 4, pp. 927–932, Aug. 2008.
[22] G. Stone, "A perspective on online partial discharge monitoring for assessment of the condition of rotating machine stator winding insulation," *IEEE Elect. Insul. Mag.*, vol. 28, no. 5, pp. 8–13, Sep. 2012.
[23] G. C. Stone, "Deterioration of stator winding insulation by vibration sparking," in *Proc. Int. Symp. Electr. Insulating Mater. (ISEIM)*, Sep. 2008, pp. 171–174.
[24] H. You, Y. Meng, and Y. Cheng, "Research on the development law of vibrating sparks on the surface of large motor bars," in *Proc. Sympos. Electr. Tech.*, 2010, pp. 1–6.

[25] R. Hartlein, "Diagnostic testing of underground cable systems (cable diagnostic focused initiative)," NEETRAC, Atlanta, GA, USA, Tech. Rep. DOE DE-FC02-04CH11237, NEETRAC 04-211/04-212/09-166, 2010.

[26] J. Densley, "Ageing mechanisms and diagnostics for power cables—An overview," *IEEE Elect. Insul. Mag.*, vol. 17, no. 1, pp. 14–22, Jan. 2001.

[27] A. Eigner and K. Rethmeier, "An overview on the current status of partial discharge measurements on AC high voltage cable accessories," *IEEE Elect. Insul. Mag.*, vol. 32, no. 2, pp. 48–55, Mar. 2016.

[28] M.-Y. Chiu, C.-H. Lee, C.-H. Huang, and S.-S. Yen, "The application of on-line PDM on in-service MV cable terminations," in *Proc. Int. Conf. Condition Monitor. Diagnosis*, 2008, pp. 1171–1174.

[29] R.-N. Wu and C.-K. Chang, "The use of partial discharges as an online monitoring system for underground cable joints," *IEEE Trans. Power Del.*, vol. 26, no. 3, pp. 1585–1591, Jul. 2011.

[30] O. Bergius, "Implementation of online partial discharge measurements in medium voltage cable network," M.S. thesis, Dept. Comput. Elect. Eng., Tampere Univ. Technol., Helsinki, Finland, 2011.

[31] T. Shahsavarian and S. M. Shahrtash, "Modelling of aged cavities for partial discharge in power cable insulation," *IET Sci., Meas. Technol.*, vol. 9, no. 6, pp. 661–670, Sep. 2015.

[32] F. Haghjoo, E. Khanahmadloo, and S. M. Shahrtash, "Comprehensive 3-capacitors model for partial discharge in power cables," *Int. J. Comput. Math. Electr. Electron. Eng.*, vol. 31, pp. 346–368, Mar. 2012.

[33] Z. Lei, J. Song, M. Tian, X. Cui, C. Li, and M. Wen, "Partial discharges of cavities in ethylene propylene rubber insulation," *IEEE Trans. Dielectr. Electr. Insul.*, vol. 21, no. 4, pp. 1647–1659, Aug. 2014.

[34] X. Chen, Y. Xu, X. Cao, S. Dodd, and L. Dissado, "Effect of tree channel conductivity on electrical tree shape and breakdown in XLPE cable insulation samples," *IEEE Trans. Dielectr. Electr. Insul.*, vol. 18, no. 3, pp. 847–860, Jun. 2011.

[35] X. Chen, Y. Xu, X. Cao, and S. M. Gubanski, "Electrical treeing behavior at high temperature in XLPE cable insulation samples," *IEEE Trans. Dielectr. Electr. Insul.*, vol. 22, no. 5, pp. 2841–2851, Oct. 2015.

[36] A. T. Bulinski, S. S. Bamji, and R. J. Densley, "Factors affecting the transition from a water tree to an electrical tree," in *Proc. Conf. Rec. IEEE Int. Symp. Electr. Insul.*, Jun. 1988, pp. 327–330.

[37] M. S. Mashikian and A. Szarkowski, "Medium voltage cable defects revealed by off-line partial discharge testing at power frequency," *IEEE Elect. Insul. Mag.*, vol. 22, no. 4, pp. 24–32, Jul. 2006.

[38] K. Zhou, M. Huang, W. Tao, M. He, and M. Yang, "A possible water tree initiation mechanism for service-aged XLPE cables: Conversion of electrical tree to water tree," *IEEE Trans. Dielectr. Electr. Insul.*, vol. 23, no. 3, pp. 1854–1861, Jun. 2016.

[39] X. Zhao, L. Pu, Z. Ju, S. Ren, W. Duan, and J. Wang, "Partial discharge characteristics and development of typical XLPE power cable insulation defects," in *Proc. Int. Conf. Condition Monitor. Diagnosis (CMD)*, Sep. 2016, pp. 623–626.

[40] C. Pan, G. Chen, J. Tang, and K. Wu, "Numerical modeling of partial discharges in a solid dielectric-bounded cavity: A review," *IEEE Trans. Dielectr. Electr. Insul.*, vol. 26, no. 3, pp. 981–1000, Jun. 2019.

[41] C. Pan, K. Wu, G. Chen, Y. Gao, M. Florkowski, Z. Lv, and J. Tang, "Understanding partial discharge behavior from the memory effect induced by residual charges: A review," *IEEE Trans. Dielectr. Electr. Insul.*, vol. 27, no. 6, pp. 1951–1965, Dec. 2020.

[42] F. Massingue, S. Meijer, P. D. Agoris, J. J. Smit, and J. Lopez-Roldan, "Partial discharge pattern analysis of modeled insulation defects in transformer insulation," in *Proc. Conf. Rec. IEEE Int. Symp. Electr. Insul.*, Jun. 2006, pp. 542–545.

[43] Y.-H. Fan, D.-G. Chang, Y.-B. Wang, and G.-J. Zhang, "Research on partial discharge identification of power transformer based on chaotic characteristics extracted by G-P algorithm," in *Proc. 2nd Int. Conf. Electr. Mater. Power Equip. (ICEMPE)*, Apr. 2019, pp. 577–581.

[44] G. Hu, G. Wu, R. Yu, P. Zhou, B. Gao, Y. Yang, and K. Liu, "The Influence of pressure on the discharge along oil-paper interface under AC stress," *Energies*, vol. 12, no. 10, pp. 1–16, 2019.

[45] X. Wang, L. Hu, and Z. Yan, "Effect of PD on the insulating paper and pressboard," *High Voltage Eng.*, vol. 27, no. 2, pp. 9–10, 2001.

[46] Y. Yuan, C. Li, Z. Zheng, S. Liu, and J. Ma, "Lab investigation of PD development in transformer winding," in *Proc. IEEE Int. Symp. Electr. Insul.*, Jun. 2010, pp. 1–4.

[47] A. Mehta, R. N. Sharma, and S. Chauhan, "Partial discharge study by monitoring key gases of power transformers," in *Proc. 3rd Int. Conf. Electron. Comput. Technol.*, vol. 4, Apr. 2011, pp. 183–186.

[48] B. H. Ward, "A survey of new techniques in insulation monitoring of power transformers," *IEEE Elect. Insul. Mag.*, vol. 17, no. 3, pp. 16–23, May 2001.

[49] K. Raja, F. Devaux, and S. Lelaidier, "Recognition of discharge sources using UHF PD signatures," *IEEE Elect. Insul. Mag.*, vol. 18, no. 5, pp. 8–14, Sep. 2002.

[50] C. Pan, J. Tang, G. Chen, Y. Zhang, and X. Luo, "Review about PD and breakdown induced by conductive particles in an insulating liquid," *High Voltage*, vol. 5, no. 3, pp. 287–297, Jun. 2020.

[51] H. Borsi and U. Schröder, "Initiation and formation of partial discharges in mineral-based insulating oil," *IEEE Trans. Dielectr. Electr. Insul.*, vol. 1, no. 3, pp. 419–425, Jun. 1994.

[52] M. G. Niasar and H. Edin, "Corona in oil as a function of geometry, temperature and humidity," in *Proc. Annu. Rep. Conf. Electr. Insul. Dielectic Phenomena (CEIDP)*, Oct. 2010, pp. 1–4.

[53] K. S. Yadav and R. Sarathi, "Influence of thermally aged barrier on corona discharge activity in transformer oil under AC voltages," *IEEE Trans. Dielectr. Electr. Insul.*, vol. 22, no. 5, pp. 2415–2423, Oct. 2015.

[54] N. A. Azrin, M. Q. Safie, M. H. Ahmad, M. A. M. Piah, M. A. B. Sidik, and Z. Nawawi, "Partial discharge characteristics of aged oil-impregnated paper under high humidity level," in *Proc. IEEE 15th Student Conf. Res. Develop. (SCOReD)*, Dec. 2017, pp. 398–401.

[55] *Partial Discharge Measurements*, document IEC 60720, 3rd ed., 2000.

[56] M. M. Mohsin, M. N. Narayanachar, and R. S. Nema, "A study of partial discharge characteristics in oil impregnated pressboard insulation," in *Proc. IEEE Int. Sympos. Electr. Insul.*, vol. 1, Jun. 1996, pp. 79–82.

[57] P. Seri, L. Cirioni, H. Naderiallaf, G. C. Montanari, R. Hebner, A. Gattozzi, and X. Feng, "Partial discharge inception voltage in DC insulation systems: A comparison with AC voltage supply," in *Proc. IEEE Electr. Insul. Conf. (EIC)*, Jun. 2019, pp. 1–4.

[58] G. C. Montanari, R. Hebner, P. Seri, and H. Naderiallaf, "Partial discharge inception voltage and magnitude in polymeric cables under AC and DC voltage supply," in *Proc. Jicable*, 2019, pp. 1–4.

[59] M. F. Rahman, B. N. Rao, and P. M. Nirgude, "Influence of moisture on partial discharge characteristics of oil impregnated pressboard under non-uniform field," in *Proc. IEEE Int. Sympos. High Voltage Eng.*, Aug. 2017, pp. 1–6.

[60] H. Shiota, H. Muto, H. Fujii, and N. Hosokawa, "Diagnosis for oil-immersed insulation using partial discharge due to bubbles in oil," in *Proc. 7th Int. Conf. Properties Appl. Dielectr. Mater.*, vol. 3, 2003, pp. 1120–1123.

[61] M. G. Niasar, H. Edin, X. Wang, and R. Clemence, "Partial discharge characteristics due to air and water vapor bubbles in oil," in *Proc. IEEE Int. Sym. High Voltage Eng.*, Aug. 2011, pp. 1–6.

[62] H. Gui and Z. De-Yi, "Surface discharge characteristics of impregnated pressboard under AC voltages," in *Proc. 3rd Int. Conf. Properties Appl. Dielectric Mater.*, 1991, pp. 313–316.

[63] P. Rozga, "Influence of paper insulation on the prebreakdown phenomena in mineral oil under lightning impulse," *IEEE Trans. Dielectr. Electr. Insul.*, vol. 18, no. 3, pp. 720–727, Jun. 2011.

[64] B. Qi, Z. Wei, and C. Li, "Creepage discharge of oil-pressboard insulation in AC-DC composite field: Phenomenon and characteristics," *IEEE Trans. Dielectr. Electr. Insul.*, vol. 23, no. 1, pp. 237–245, Feb. 2016.

[65] F. Murdiya, R. Hanaoka, H. Akiyama, K. Miyagi, K. Takamoto, and T. Kano, "Creeping discharge developing on vegetable-based oil/pressboard interface under AC voltage," *IEEE Trans. Dielectr. Electr. Insul.*, vol. 21, no. 5, pp. 2102–2110, Oct. 2014.

[66] J. Li, W. Si, X. Yao, and Y. Li, "Partial discharge characteristics over differently aged oil/pressboard interfaces," *IEEE Trans. Dielectr. Electr. Insul.*, vol. 16, no. 6, pp. 1640–1647, Dec. 2009.

[67] H. Jahangir, A. Akbari, P. Werle, M. Akbari, and J. Szczechowski, "UHF characteristics of different types of PD sources in power transformers," in *Proc. Iranian Conf. Electr. Eng. (ICEE)*, May 2017, pp. 1242–1247.

[68] P. M. Mitchinson, P. L. Lewin, B. D. Strawbridge, and P. Jarman, "Tracking and surface discharge at the oil-pressboard interface," *IEEE Electr. Insul. Maga.*, vol. 26, no. 2, pp. 35–41, Jun. 2010.

[69] X. Yi and Z. Wang, "Surface tracking on pressboard in natural and synthetic transformer liquids under AC stress," *IEEE Trans. Dielectr. Electr. Insul.*, vol. 20, no. 5, pp. 1625–1634, Oct. 2013.

[70] V. Sokolov, Z. Berler, and V. Rashkes, "Effective methods of assessment of insulation system conditions in power transformers: A view based on practical experience," in *Proc. Electr. Insul. Conf. Electr. Manuf. Coil Winding Conf.*, Cincinnati, OH, USA, 1999, pp. 659–667.
[71] R. Eberhardt, H. M. Muhr, W. Lick, B. Wieser, R. Schwarz, and G. Pukel, "Partial discharge behaviour of an alternative insulating liquid compared to mineral oil," in *Proc. IEEE Int. Power Modulator High Voltage Conf.*, May 2010, pp. 1–4.
[72] J. B. DiGiorgio, "Dissolved gas analysis of mineral oil insulating fluids," Northern Technol. Test., Sacramento, CA, USA. [Online]. Available: http://www.nttworldwide.com
[73] I. A. Metwally, "Technology progress in high-voltage gas-insulated substations," *IEEE Potentials*, vol. 29, no. 6, pp. 25–32, Nov. 2010.
[74] W. G. Cigre, "Insulation coordination of GIS: Return of experience, on site tests and diagnostic techniques," *Electra*, no. 176, pp. 67–95, Feb. 1998.
[75] U. Schichler, W. Koltunowicz, F. Endo, K. Feser, A. Giboulet, A. Girodet, H. Hama, B. Hampton, H.-G. Kranz, J. Lopez-Roldan, L. Lundgaard, S. Meijer, C. Neumann, S. Okabe, J. Pearson, R. Pietsch, U. Riechert, and S. Tenbohlen, "Risk assessment on defects in GIS based on PD diagnostics," *IEEE Trans. Dielectr. Electr. Insul.*, vol. 20, no. 6, pp. 2165–2172, Dec. 2013.
[76] Y. Wang, J. Li, H. Liang, H. Yu, and X. Zhao, "Characteristic analysis of partial discharge detection in GIS," *Int. J. Digit. Content Technol. Appl.*, vol. 6, no. 18, p. 482, 2012.
[77] J. Tang, J. Tao, X. Zhang, and J. Zhou, "Investigation of partial discharge on typical defects with UHF detection method for GIS," *Przeglad Elektrotechniczny*, vol. 88, pp. 351–355, Jan. 2012.
[78] F. Zeng, J. Tang, X. Zhang, S. Zhou, and C. Pan, "Typical internal defects of gas-insulated switchgear and partial discharge characteristics," in *Simulation and Modelling of Electrical Insulation Weaknesses in Electrical Equipment*, R. A. Sanchez, Ed. U.K.: IntechOpen, 2018, pp. 103–128.
[79] A. Darwish, S. S. Refaat, H. A. Toliyat, and H. Abu-Rub, "On the electromagnetic wave behavior due to partial discharge in gas insulated switchgears: State-of-art review," *IEEE Access*, vol. 7, pp. 75822–75836, 2019.
[80] X. Zhang, H. Liu, J. Ren, J. Li, and X. Li, "Fourier transform infrared spectroscopy quantitative analysis of SF6 partial discharge decomposition components," *Spectrochimica Acta A, Mol. Biomolecular Spectrosc.*, vol. 136, pp. 884–889, Feb. 2015.
[81] Z. An, F. Liu, Y. Tang, F. Zheng, and Y. Zhang, "Resistance of surface fluorinated epoxy resin to corona discharge in SF_6 gas," *IEEE Trans. Dielectr. Electr. Insul.*, vol. 23, no. 6, pp. 3659–3667, Dec. 2016.
[82] S. Wu, F. Zeng, J. Tang, Q. Yao, and Y. Miao, "Triangle fault diagnosis method for SF_6 gas-insulated equipment," *IEEE Trans. Power Del.*, vol. 34, no. 4, pp. 1470–1477, Aug. 2019.
[83] J. Li, X. Han, Z. Liu, and X. Yao, "A novel GIS partial discharge detection sensor with integrated optical and UHF methods," *IEEE Trans. Power Del.*, vol. 33, no. 4, pp. 2047–2049, Aug. 2018.
[84] M. Hikita, S. Ohtsuka, and S. Matsumoto, "Recent trend of the partial discharge measurement technique using the UHF electromagnetic wave detection method," *IEEJ Trans. Electr. Electron. Eng.*, vol. 2, no. 5, pp. 504–509, 2007.
[85] M. Hikita, S. Okabe, H. Murase, and H. Okubo, "Cross-equipment evaluation of partial discharge measurement and diagnosis techniques in electric power apparatus for transmission and distribution," *IEEE Trans. Dielectr. Electr. Insul.*, vol. 15, no. 2, pp. 505–518, Apr. 2008.
[86] S. Meijer and J. J. Smit, "UHF defect evaluation in gas insulated equipment," *IEEE Trans. Dielectr. Electr. Insul.*, vol. 12, no. 2, pp. 285–296, Apr. 2005.
[87] K. Dreisbusch, H.-G. Kranz, and A. Schnettler, "Determination of a failure probability prognosis based on PD–diagnostics in gis," *IEEE Trans. Dielectr. Electr. Insul.*, vol. 15, no. 6, pp. 1707–1714, Dec. 2008.
[88] G. C. Stone, S. R. Campbell, and H. Sedding, "Applicability of partial discharge testing for 4 kV motor and generator stator windings," in *Proc. Elect. Electron. Insul. Conf. Electr. Manuf. Coil Winding Conf.*, 1995, pp. 665–668.
[89] G. C. Stone, T. E. Goodeve, H. G. Sedding, and W. McDermid, "Unusual PD pulse phase distributions in operating rotating machines," *IEEE Trans. Dielectr. Electr. Insul.*, vol. 2, no. 4, pp. 567–577, Aug. 1995.
[90] M. Fenger, E. Goodeve, and V. Warren, "Distinguishing between specific deterioration phenomena in stator windings and cross coupled PD," in *Proc. Annu. Rep. Conf. Electr. Insul. Dielectr. Phenomena*, vol. 2, 2000, pp. 582–586.
[91] Z. Ma, C. Zhou, D. M. Hepburn, and K. Cowan, "Fractal theory based pattern recognition of motor partial discharge," in *Proc. Int. Conf. Condition Monitor. Diagnosis (CMD)*, Sep. 2016, pp. 881–884.
[92] M. Tozzi, G. C. Montanari, D. Fabiani, A. Cavallini, and G. Gao, "Off-line and on-line PD measurements on induction motors fed by power electronic impulses," in *Proc. IEEE Electr. Insul. Conf.*, May 2009, pp. 420–424.
[93] D. W. Gross, "On-line partial discharge diagnosis on large motors," in *Proc. Annu. Rep. Conf. Electr. Insul. Dielectr. Phenomena*, 2002, pp. 474–477.
[94] G. C. Stone and V. Warren, "Objective methods to interpret partial-discharge data on rotating-machine stator windings," *IEEE Trans. Ind. Appl.*, vol. 42, no. 1, pp. 195–200, Jan. 2006.
[95] G. C. Stone, "Relevance of phase resolved PD analysis to insulation diagnosis in industrial equipment," in *Proc. 10th IEEE Int. Conf. Solid Dielectr.*, Jul. 2010, pp. 1–5.
[96] A. Contin, M. Aizza, F. Fantin, and A. Piccolo, "Identification of PD sources and insulation technologies in rotating machines," in *Proc. IEEE Electr. Insul. Conf. (EIC)*, Aug. 2015, pp. 458–462.
[97] A. Krivda and S. Halen, "Recognition of PD patterns in generators," in *Proc. 5th Int. Conf. Properties Appl. Dielectr. Mater.*, 1997, pp. 206–211.
[98] C. Hudon, N. Amyot, M. Levesque, M. Essalihi, and C. Millet, "Using integrated generator diagnosis to perform condition based maintenance," in *Proc. IEEE Electr. Insul. Conf. (EIC)*, Aug. 2015, pp. 341–345.
[99] H. D. Kim and Y. H. Ju, "Measurement and analysis of partial discharge in high voltage motor stator windings," in *Proc. Electr. Insul. Conf. Electr. Manuf. Coil Winding Technol. Conf.*, 2003, pp. 27–31.
[100] H. D. Kim and Y. H. Ju, "Comparison of off-line and on-line partial discharge for large motors," in *Proc. Conf. Rec. the IEEE Int. Symp. Electr. Insul.*, Apr. 2002, pp. 27–30.
[101] M. Levesque, C. Hudon, and E. David, "Insulation degradation analysis of stator bars subjected to slot partial discharges," in *Proc. IEEE Electr. Insul. Conf. (EIC)*, Jun. 2013, pp. 479–483.
[102] G. C. Stone, V. Warren, and M. Fenger, "Case studies on the effect of humidity on stator winding partial discharge activity," in *Proc. Conf. Rec. the IEEE Int. Symp. Electr. Insul.*, Apr. 2002, pp. 579–581.
[103] C. Azuaje and W. Torres, "Experiences in identification of partial discharge patterns in large hydrogenerators," in *Proc. IEEE/PES Transmiss. Distrib. Conf. Expo., Latin Amer.*, Aug. 2006, pp. 1–6.
[104] G. C. Stone and V. Warren, "Effect of manufacturer, winding age and insulation type on stator winding partial discharge levels," *IEEE Elect. Insul. Mag.*, vol. 20, no. 5, pp. 13–17, Sep. 2004.
[105] G. C. Stone, E. A. Boulter, I. Culbert, and H. Dhirani, *Electrical Insulation for Rotating Machines: Design, Evaluation, Aging, Testing, and Repair*, 2nd ed. Hoboken, NJ, USA: Wiley, 2014.
[106] M. Levesque, E. David, C. Hudon, and M. Belec, "Contribution of humidity to the evolution of slot partial discharges," *IEEE Trans. Dielectr. Electr. Insul.*, vol. 19, no. 1, pp. 61–75, Feb. 2012.
[107] M. Bélec and C. Hudon, "Long term aging test on stator bars exposed to end arm discharges," in *Proc. Annu. Rep. Conf. Electr. Insul. Dielect. Phenom. (CEIDP)*, 1998, pp. 550–554.
[108] M. Fenger and G. C. Stone, "Investigation of the effect of humidity on partial discharge activity in stator windings," in *Proc. 7th Int. Conf. Properties Appl. Dielectr. Mater.*, 2003, pp. 1080–1083.
[109] M. Fenger, G. C. Stone, and B. A. Lloyd, "The impact of humidity on PD inception voltage as a function of rise-time in random wound motors of different designs," in *Proc. Annu. Rep. Conf. Electr. Insul. Dielectr. Phenomena*, 2002, pp. 501–505.
[110] M. Levesque, E. David, and C. Hudon, "Effect of surface conditions on the electric field in air cavities," *IEEE Trans. Dielectr. Electr. Insul.*, vol. 20, no. 1, pp. 71–81, Feb. 2013.
[111] M. Fenger and G. C. Stone, "How humidity affects partial discharge activity in stator windings," in *Proc. Electr. Insul. Conf. Electr. Manuf. Coil Winding Technol. Conf.*, 2003, pp. 47–50.
[112] L. Lin, A. Kang, J. Song, Z. Lei, Y. Zhao, and A. Isenberg, "Effect of water vapor on oil-contamination discharge of stator windings," in *Proc. IEEE Int. Conf. Dielectr. (ICD)*, Jul. 2016, pp. 642–645.
[113] K. Wu, M. Kanegami, T. Takahashi, H. Suzuki, T. Ito, T. Okamoto, and H. Yano, "Influence of mechanical vibration on the behavior of partial discharges in generator stator windings," in *Proc. Int. Symp. Electr. Insulating Mater. (ISEIM)*, vol. 1, 2005, pp. 281–284.
[114] C. Hudon and M. Belec, "Aging of stator bars exposed to end arm discharges," in *Proc. Conf. Electr. Insul. Dielectr. Phenomena (CEIDP)*, vol. 2, 1996, pp. 829–832.

[115] A. Cavallini, G. C. Montanari, F. Puletti, and A. Contin, "A new methodology for the identification of PD in electrical apparatus: Properties and applications," *IEEE Trans. Dielectr. Electr. Insul.*, vol. 12, no. 2, pp. 203–215, Apr. 2005.
[116] C. Suwanasri, T. Sangpakdeejit, N. Vipulum, P. Fuangpian, S. Ruankon, and T. Suwanasri, "Investigation on partial discharge inception voltage and discharge pattern of simulated defect cable system," in *Proc. Int. Conf. Condition Monitor. Diagnosis (CMD)*, Xi'an, China, Sep. 2016, pp. 238–241.
[117] Y. Li, Z. Lei, L. Li, J. Song, J. Zeng, Y. Li, and X. Xu, "Characteristics of flashover and discharge over the surface of ethylene propylene rubber," in *Proc. Int. Conf. Condition Monitor. Diagnosis (CMD)*, Xi'an, China, Sep. 2016, pp. 1024–1027.
[118] D. Fynes-Clinton and C. Nyamupangedengu, "Partial discharge characterization of cross-linked polyethylene medium voltage power cable termination defects at very low frequency (0.1 Hz) and power frequency test voltages," *IEEE Elect. Insul. Mag.*, vol. 32, no. 4, pp. 15–23, Jul. 2016.
[119] R. Candela, G. F. Scimemi, P. Romano, and E. R. Sanseverino, "Analysis of partial discharge activity at different temperatures through an heuristic algorithm," in *Proc. Annu. Rep. Conf. Electr. Insul. Dielectr. Phenomena*, 1999, pp. 202–205.
[120] L. Wang, A. Cavallini, G. C. Montanari, and L. Testa, "Evolution of pd patterns in polyethylene insulation cavities under AC voltage," *IEEE Trans. Dielectr. Electr. Insul.*, vol. 19, no. 2, pp. 533–542, Apr. 2012.
[121] C. S. Kim, T. Kondo, and T. Mizutani, "Change in PD pattern with ageing," *IEEE Trans. Dielectr. Electr. Insul.*, vol. 11, pp. 13–18, 2004.
[122] P. H. F. Morshuis, "Degradation of solid dielectrics due to internal partial discharge: Some thoughts on progress made and where to go now," *IEEE Trans. Dielectr. Electr. Insul.*, vol. 12, no. 5, pp. 905–913, Oct. 2005.
[123] X. Zhu, J. Wu, Y. Wang, and Y. Yin, "Characteristics of partial discharge and AC electrical tree in XLPE and MgO/XLPE nanocomposites," *IEEE Trans. Dielectr. Electr. Insul.*, vol. 27, no. 2, pp. 450–458, Apr. 2020.
[124] B. Du, T. Ma, J. Su, M. Tian, T. Han, and X. Kong, "Effects of temperature gradient on electrical tree growth and partial discharge in silicone rubber under AC voltage," *IEEE Access*, vol. 8, pp. 54009–54018, 2020.
[125] S. Azizi-Ghannad and J. K. Nelson, "Artificial intelligence applied to the aging of machine insulation," in *Proc. Annu. Rep. Conf. Electr. Insul. Dielectric Phenomena*, vol. 2, 1998, pp. 534–537.
[126] S. Senthil Kumar, M. N. Narayanachar, and R. S. Nema, "Pulse sequence studies on PD data," in *Proc. Annu. Rep. Conf. Electr. Insul. Dielectric Phenomena*, 2002, pp. 724–727.
[127] M. Pompili, C. Mazzetti, and R. Bartnikas, "PD pulse burst characteristics of transformer oils," *IEEE Trans. Power Del.*, vol. 21, no. 2, pp. 689–698, Apr. 2006.
[128] N. D. Jacob and W. M. McDermid, "Experience with partial discharge measurements on instrument transformers in high voltage laboratory acceptance tests," in *Proc. PES T D*, May 2012, pp. 1–4.
[129] A. Cavallini, G. C. Montanari, and F. Ciani, "Analysis of partial discharge phenomena in paper-oil insulation systems as a basis for risk assessment evaluation," in *Proc. IEEE Int. Conf. Dielectric Liquids (ICDL)*, Jun. 2005, pp. 241–244.
[130] S. Y. Matharage, Q. Liu, and Z. D. Wang, "Aging assessment of kraft paper insulation through methanol in oil measurement," *IEEE Trans. Dielectr. Electr. Insul.*, vol. 23, no. 3, pp. 1589–1596, Jun. 2016.
[131] X. Yi and Z. Wang, "Creepage discharge on pressboards in synthetic and natural ester transformer liquids under AC stress," *IET Electr. Power Appl.*, vol. 7, no. 3, pp. 191–198, Mar. 2013.
[132] R. Piccin, A. Mor, P. Morshuis, A. Girodet, and J. Smit, "Partial discharge analysis of gas insulated systems at high voltage AC and DC," *IEEE Trans. Dielectr. Electr. Insul.*, vol. 22, no. 1, pp. 218–228, Feb. 2015.
[133] X. Shao, W. He, J. Xu, M. Zhu, and G. Zhang, "Partial discharge detection by extracting UHF signal from inner grading electrode of insulating spacer in GIS," *IET Sci., Meas. Technol.*, vol. 12, no. 1, pp. 90–97, Jan. 2018.
[134] M. T. Nguyen, V. H. Nguyen, S. J. Yun, and Y. H. Kim, "Recurrent neural network for partial discharge diagnosis in gas-insulated switchgear," *Energies*, vol. 11, p. 1202, May 2018.
[135] R. Yao, Y. Zhang, G. Si, Y. Yuan, and Q. Xie, "Measurement and analysis of partial discharge on floating electrode defect in GIS," in *Proc. IEEE Int. Conf. High Voltage Eng. Appl. (ICHVE)*, Sep. 2016, pp. 1–4.
[136] J. Tang, M. Jin, F. Zeng, S. Zhou, X. Zhang, Y. Yang, and Y. Ma, "Feature selection for partial discharge severity assessment in gas-insulated switchgear based on minimum redundancy and maximum relevance," *Energies*, vol. 10, no. 10, p. 1516, Oct. 2017.
[137] Z. Wu, Q. Zhang, J. Ma, X. Li, and T. Wen, "Effectiveness of on-site dielectric test of GIS equipment," *IEEE Trans. Dielectr. Electr. Insul.*, vol. 25, no. 4, pp. 1454–1460, Aug. 2018.
[138] J. Yang, W. Shi, H. T. Li, B. Gong, and W. Y. Jiang, "Analysis of partial discharge ultrasonic wave characteristic on typical defects in GIS," in *Proc. MATEC Web Conf.*, 2016, p. 01017.
[139] S. Xianjun, L. Feiran, C. Xiaoxin, W. Ziling, M. Bingxiao, and H. Wenlin, "Detection and diagnosis of multiple-void discharge sources in on-site 550kV GIS insulating spacer," in *Proc. 2nd Int. Conf. Electr. Mater. Power Equip. (ICEMPE)*, Apr. 2019, pp. 605–610.
[140] X. Zhang, J. Ren, J. Tang, and C. Sun, "Kernel statistical uncorrelated optimum discriminant vectors algorithm for GIS PD recognition," *IEEE Trans. Dielectr. Electr. Insul.*, vol. 16, no. 1, pp. 206–213, Feb. 2009.
[141] X. Zhang, S. Xiao, N. Shu, J. Tang, and W. Li, "GIS partial discharge pattern recognition based on the chaos theory," *IEEE Trans. Dielectr. Electr. Insul.*, vol. 21, no. 2, pp. 783–790, Apr. 2014.

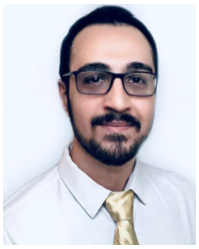

TOHID SHAHSAVARIAN received the bachelor's degree in electrical engineering from the University of Tabriz, in 2011, and the master's degree from the University of Science and Technology at Meghalaya (IUST), in 2013. He is currently pursuing the Ph.D. degree with the Department of Electrical and Computer Engineering, University of Connecticut. Then, he worked with the Department of Transmission and Distribution, Monenco Iran Consulting Engineers Company. His research interests include the partial discharge analysis and risk assessment of AC and DC power cables, enhancement of insulation performance in electrical and electronic components for aerospace application, reliability analysis and protection of HVAC/HVDC grids, and geomagnetic disturbances (GMD).

YUE PAN was born in Shanghai, China, in 1995. She received the B.S. degree in electrical engineering from the Shanghai University of Electric Power, Shanghai, in 2018, where she is currently pursuing the master's degree in electrical engineering. Her research interest includes the on-line monitoring of electrical insulation of power equipment.

ZHOUSHENG ZHANG was born in Enshi City, China, in 1969. He received the B.S. degree in physics from Huazhong Normal University, in 1992, the M.S. degree in electrical engineering from the Huazhong University of Science and Technology, in 1999, and the Ph.D. degree in electrical engineering from Shanghai Jiao Tong University, in 2010. He is currently a Professor with the Shanghai University of Electric Power. His current research interests include gas discharges, electrical insulation and materials, and condition monitoring of power apparatus.

CHENG PAN (Member, IEEE) was born in Guangshui, China, in 1986. He received the B.S. and Ph.D. degrees in electrical engineering from Xi'an Jiaotong University, China, in 2008 and 2014, respectively. Then, he joined State Grid of China, as a Transformer Engineer. After 2015, he became a Lecturer with Wuhan University, China, where he also held a postdoctoral position. From 2017 to 2018, he was with the Tony Davies High Voltage Laboratory, University of Southampton. His research interests include partial discharge mechanism, surface charge accumulation at dc voltage, and breakdown characteristics of moving transformer oil.

HADI NADERIALLAF (Member, IEEE) was born in Mashhad, Iran, in April 1986. He received the M.Sc. degree in electrical engineering from Leibniz Universität Hannover, Germany, in 2012. He is currently pursuing the Ph.D. degree with the University of Bologna, Italy. He was working on the EU project GRIDABLE, during the Ph.D. degree. He did his master thesis at the Schering Institute of High Voltage Techniques and Engineering, Leibniz Universität Hannover. He has working experience for five years, as a Transformer Fluid Specialist. His research interests include liquid and nanostructured solid electrical insulating materials, HVDC cables design, space charge measurement and analysis, AC and DC partial discharge detection and modeling, insulation systems for electrical machines, condition monitoring techniques, HV transformer asset management, and DGA and transformer oil reclamation.

JIM GUO (Senior Member, IEEE) received the B.A. and M.Sc. degrees in electrical engineering from the School of Electrical Engineering, Southwest Jiaotong University, Sichuan, China, in 2003 and 2006, respectively, and the Ph.D. degree in material science from the Electrical Insulation Research Center, Institute of Material Science, University of Connecticut, Storrs, CT, USA, in 2010. From 2010 to 2015, he was with UtilX Corporation, as an Engineering Systems Analyst and a Project Manager. Since 2015, he has been with Techimp U.S. Corporation, as a VP of technology. He has over ten years of experiences working in the field of diagnostic testing for high voltage apparatus. He has more than 30 publications in peer reviewed journals and international conferences, and holds four U.S. and international patents. His research interests include high voltage dielectric aging and breakdown theories, partial discharge measurement and analysis under unconventional waveforms, and partial discharge signal processing and automation. He is currently a Senior Member of the PES Insulated Conductor Committee (ICC) working in several power cable standard committees. He serves as the Co-Chair for the Chapter/the Membership Committee in IEEE-DEIS. He is a frequent reviewer for multiple IEEE and IET journals, and serves as an Associate Editor for *IET Science Measurement and Technology*.

CHUANYANG LI received the Ph.D. degree from the Department of Electrical Engineering, Tsinghua University, in 2018. From 2018 to 2019, he worked as a Postdoctoral Fellow with the Department of Electrical, Electronic, and Information Engineering "Guglielmo Marconi," University of Bologna, Italy. Since November 2019, he has been working with the Department of Electrical and Computer Engineering, and the Institute of Materials Science, University of Connecticut, as a Postdoctoral Fellow. His research interests include surface charge behavior and modification methods and PD properties of high temperature material in harsh conditions. He served as a Lead Guest Editor for the IEEE TRANSACTIONS ON DIELECTRICS AND ELECTRICAL INSULATION Special Issue on Advanced Dielectrics for Gas-Insulated Transmission Lines, in 2018 and *Nanotechnology* Focus Collection on Focus on Gas-Solid Interface Charging Physics, in 2020, and a Guest Editor for *High Voltage* Special Issue on Interface Charging Phenomena for Dielectric Materials. He is currently an Associate Editor of *High Voltage* (IET).

YANG CAO (Senior Member, IEEE) received the B.S. and M.S. degrees in physics from Tongji University, Shanghai, China, and the Ph.D. degree from the University of Connecticut, in 2002. He served as a Senior Electrical Engineer for the GE Global Research Center, in 2013. He is currently a Full Professor with the Department of Electrical and Computer Engineering, University of Connecticut. He is also the Director of the Electrical Insulation Research Center, Institute of Materials Science, and the Site Director of the NSF iUCRC Center on High Voltage/Temperature Materials and Structures. His research interests include the physics of materials under extremely high field and the development of new dielectric materials, particularly the polymeric nanostructured materials, for energy efficient power conversion and renewables integrations, and for novel medical diagnostic imaging devices.